A STUDY ON HALLOYSITE REINFORCED CHITOSAN HYDROGEL NANOCOMPOSITES: SYNTHESIS, CHARACTERIZATION & DYE ADSORPTION PROPERTIES

by

Sinem PALANTÖKEN

B.S., Chemistry, Bilkent University, 2013

Submitted to the Institute for Graduate Studies in
Science and Engineering in partial fulfillment of
the requirements for the degree of
Master of Science

Graduate Program in Chemistry

Boğaziçi University

2015

A STUDY ON HALLOYSITE REINFORCED CHITOSAN HYDROGEL NANOCOMPOSITES: SYNTHESIS, CHARACTERIZATION & DYE ADSORPTION PROPERTIES

APPROVED BY:

Prof. Nihan Nugay …….……
(Thesis Supervisor)

Assoc. Prof. Sinan Şen …….……

Assist. Prof. Fırat İlker …….……

DATE OF APPROVAL: 30/04/2015

To my mom, dad and Cancanık

ACKNOWLEDGEMENTS

First of all, I would like to thank Prof. Nihan Nugay for giving me the chance of being a part of their research group and teaching me during the project and also thank to Prof. Turgut Nugay for his guidance in experimenting.

I would also thank to my committee members Assoc. Prof. Sinan Şen for colloborating and making guiding comments through the project and for being one of the member of my examining committee. Also, I sincerely thank to Assist. Prof. Fırat İlker for his careful reviewing of my thesis.

I would like to express my special thanks to Bilge Gedik Uluocak for her valuable help in ESEM and EDX measurements and also Muhammed Erkan Karabekmez for XRD measurement. I would like to thank to Emre Tekay from Yalova University Polymer Engineering Department for Compression Testing measurements. Also we appreciate Turgay Gönül at Sabancı University for helping in TEM based characterization.

I would also thank to my lab friends. Special thanks to Ekmel for his patience for answering all of my questions, Çimen for her endless support and Elif for her friendship. It was great pleasure for me to work with them.

I will always remember the support of all of my friends. I would give my special thanks to my friends Aylin Aykanat, Duygu Baykal, Ozan Özdemir, Ayşenur Özdemir, Ece Çiftçi, Gamze Bahadır, Tuğçe Erbay, Taner Özden and Derya Melis Karagöz.

Finally, I would also thank to my family, mum, dad and my brother Can for their unconditional support and encouragement during all my life.

Lastly, thanks to Eczacıbaşı ESAN for donating Halloysite nanotubes to this project and thanks to Scientific Research Department of Boğaziçi University for financial support with project no: 14B05P2.

ABSTRACT

A STUDY ON HALLOYSITE REINFORCED CHITOSAN HYDROGEL NANOCOMPOSITES: SYNTHESIS, CHARACTERIZATION and DYE ADSORPTION PROPERTIES

In this project, synthesis and characterization of a series of natural silica nanotube reinforced chitosan nanocomposite hydrogels are done. Nanocomposite hydrogels were prepared through physical crosslinking of chitosan and within different percentages of Halloysite nanotube (HNTs) reinforcement. To increase the surface activity of halloysite nanotubes without disturbing the tubular structure, a special modification based on cryoscopic expansion was conducted and modification success was confirmed by X-Ray Diffraction, Brunauer-Emmett-Teller and Scanning Electron Microscope analysis methods. It has been found that both inner and outer diameters as well as surface area of nanotubes can be increased efficiently without disturbing the inherent tubular structure. Hydrogel nanocomposites were then prepared with different percentages of original and modified halloysite nanotubes and -their water absorption, mechanical and dye adsorption properties as well as morphologies were investigated with a special focus on lumen modification and loading degree. Compared to neat hydrogels, swelling and mechanical properties of the composite hydrogels were found to be enhanced because of special morphology devolopment depending on composition. This effect was observed in a distinct way when cryo-expanded halloysite nanotubes were considered. Besides that neat chitosan turns out to be a good adsorbent for anionic dye; if small amount of cryo-expanded halloysite is added into the composition, the resultant composite hydrogel displays not only high adsorption capacity for both anionic and cationic type of dyes but also better mechanical properties.

ÖZET

HALLOYSİT İLE GÜÇLENDİRİLMİŞ HİDROJEL NANOKOMPOZİTLERİ ÜZERİNE BİR ÇALIŞMA: SENTEZ, KARAKTERİZASYON ve BOYA TUTMA KAPASİTESİ ÖZELLİKLERİ

Bu projede, bir dizi doğal silika nanotüp destekli Kitosan hidrojel nanokompozitlerinin sentez ve karakterizasyon çalışmaları öngörülmüştür. Nanokompozit hidrojeller, halloysit nanotüp (HNT) dolgusunun farklı yüklemeleri varlığında, kitosan doğal polimerinin fiziksel çapraz bağlanmasıyla hazırlandı. Halloysit nanotüplerinin tüp yapısını bozmadan yüzey aktivitesini artırmak için kriyoskopik genişlemeye bağlı bir modifikasyon yöntemi uygulanmıştır ve modifikasyonun başarılı olduğu, X-Işını Kırılımı (XRD), Brunauer-Emmett-Teller (BET) ve Elektron Taramalı Mikroskopi (SEM) analiz yöntemleriyle doğrulanmıştır. Nanotüplerin kendi tüp yapısını bozmadan iç ve dış çaplarında olduğu gibi yüzey alanının da etkili bir biçimde arttığı gözlemlenmiştir. Daha sonra orijinal ve modifiye Halloysit nanotüp varlığında elde edilen nanokompozit hidrojellerinin su tutma kapasitesi, mekanik davranımları ve boya tutma kapasitelerinin yanısıra morfolojileri; tüp lümen boşluğunun modifikasyonu ve dolgulama yüzdesine bağlı olarak araştırılmıştır. Saf kitosan hidrojelleriyle kıyaslandığında, bileşimine dayalı özel morfolojik gelişme sayesinde kompozit hidrojellerin şişme ve mekanik özelliklerinin iyileştiği gözlemlenmiştir. Bu gelişme, kriyo-genişletilmiş halloysit nanotüpleri söz konusu olduğunda daha da belirgin bir biçimde gözlemlenmiştir. Saf kitosan hidrojelinin taşıdığı yük ile bağlantılı olarak anyonik boyalar için çok etkin bir emici madde olmasının gözlemlenmesinin yanısıra; eğer bileşime az miktarda özel kriyo-genişletilmiş halloysit eklenirse ortaya çıkan hidrojel hem anyonik hem katyonik boyalar için yüksek boya tutma kapasitesine sahip olmanın dışında mekanik dayanımında da iyileşme sergileyebilmektedir.

TABLE OF CONTENTS

LIST OF FIGURES

LIST OF TABLES

LIST OF ACRONYMS/ABBREVIATIONS

AA	Acetic acid
APTES	γ-aminopropyltriethoxysilane
APTMS	N-(β-aminoethyl)-γ-aminopropyltrimethoxysilane
BCG	Bromocresol Green
BET	Brunauer-Emmett-Teller
CH	Chitosan
CNTs	Carbon nanotubes
CO	Castor Oil
CR	Congo Red
DD	Degree of Deacetylation
DNA	Deoxy Ribonucleic Acid
EB	Electron Beam
EDX	Electron Dispersive X-Ray Spectroscopy
EGDMA	Ethylene glycol dimethacrylate
FDA	Food and Drug Administration
FTIR	Fourier Transform Infrared Radiation
GEL	Gelatin
GRAS	Generally Recognized As Safe
HAp	Hydroxyapatite
HEMA	2-Hydroxy ethyl methacrylate
HL	Halloysite
HLCH	Chitosan-Halloysite nanocomposite hydrogels
HNTs	Halloysite nanotubes
HPMC	Hydroxypropylmethylcellulose
LCST	Lower Critical Solution Temperature
MAA	Methacrylic acid
M-HNTs	Modified Halloysite nanotubes
MMT	Montmorillonite
MO	Methyl Orange

NB	Nile Blue
NIPAM	N-isopropylacrylamide
PAN	Poly(acrylonitrile)
PD	Poly(N,N'-dimethylacrylamide)
PEG	Poly(ethylene glycol)
$POCl_3$	Phosphorous oxychloride
POM	Polar polyoxymethylene
PP	Polypropylene
PPA	Phenylphosphonic acid
PVA	Poly(vinyl alcohol)
SA	Sodium alginate
SEM	Scanning Electron Microscope
TEM	Transmission Electron Microscopy
TGA	Thermal Gravimetric Analysis
TPP	Sodium tripolyphate
TPT	Oligo(trimethylene carbonate)-poly(ethylene glycol)- oligo (trimethylene carbonate)-diacrylate
UV-Vis	Ultraviolet-Visible analysis
WSC	Water Soluble Chitosan
XPHL	Expanded form of halloysite
XPHLCH	Chitosan-Cryo Expanded Halloysite nanocomposite hydrogels
XRD	X-Ray Diffraction

LIST OF SYMBOLS

%/^{o}C	Derivative weight change
% (v/v)	Volume-Volume Percentage
C	Concentration
°C	Degrees Celcius
c_0	Initial concentration of dye
c_i	Equilibrium concentration of dye
Da	Dalton
g	Gram
h	Hour
L	Liter
min	Minute
mg	Miligram
ml	Millilitre
µ	Micron
µm	Micrometer
M	Molar
M_w	Weight Average Molecular Weight
MW	Molecular Weight
nm	Nanometer
P	Pressure
RT	Room Temperature
q	Amount of the dye adsorbed onto the unit amount of the hydrogel
T	Temperature
T_{d50}	Degradation temperature at mid-point
T_{d20}	Degradation temperature when 20% of the sample is lost
V	Volume
V_{pore}	Pore Volume
wt%	Weight Percentage
W	Weight of the hydrogel

1. INTRODUCTION

1.1. Hydrogels

Hydrogels are three-dimensional hydrophilic network structures having a high absorption capacity of aqueous solutions [1]. Hydrogels are stimulated by pH, ionic strength, solvent composition, light and electric field. These features help hydrogels serve in tissue engineering, enzyme biosensor, drug delivery, chemical valves, dye adsorption, agriculture and catalysis.

Hydrogels are classfied as covalently (chemically) or ionically (physically) crosslinked hydrogels in terms of crosslinking [1]. If there occurs a permanent network structure during the hydrogel formation, the hydrogel is chemically crosslinked; whereas physically crosslinked hydrogels have momentary junctions which result from entanglements of polymer chains or physical interactions like ionic/hydrophobic interactions or hydrogen/Van der Waals bonds [2].

There are covalent bonds between different polymer chains of chemically crosslinked hydrogels. They are stable until the covalent crosslink points are cleaved [3]. Examples of crosslinking agents used for hydrogels include ethylene glycol dimethacrylate (EGDMA) [4], tetrafunctional N,N'-methylene bis-acrylamide and octafunctional glyoxal bis(dially acetal) (GLY) [5].

Avoiding the use of crosslinking agents becomes useful in pharmaceutical applications for the toxic properties seen in some of the crosslinked hydrogels. Kamoun *et al.* blended aqueous solution of sodium alginate (SA) with poly(vinyl alcohol) and continued with physical crosslinking using freeze-thawing method instead of chemical crosslinking agents to avoid chemical reagents. They obtained PVA-SA hydrogels containing a topical antibiotics for wound dressing applications [6]. In another study, Niu *et al.* obtained physically crosslinked hydrogels by immersing compression-molded

hydrophobic/hydrophilic poly(2-(N-ethylperfluorooctanesulfonamido) ethylmethyl acrylate) and poly(N,N'-dimethylacrylamide) (PD) triblock copolymers into water [7].

There are several methods to prepare hydrogels. Solution and inverse solution suspension polymerizations are used for preparation of the hydrogel composites and hydrogel nanocomposites [3]. Hydrogels can also be prepared by radiation treatment. It can be ionizing, gamma rays or electron beam radiation. For radiation treatment, no crosslinking agent or initiator is required. The reaction can be done at room temperature [8]. Güven *et al.* used hydroxypropylmethylcellulose (HPMC) with different degrees of substitution, and irradiated this polymer with electron beam (EB) radiation at ambient temperatures, various doses and concentrations [8]. It was found that gel content increases when radiation dose increases or HPMC concentration decreases. HPMC gels seem to be temperature-sensitive hydrogels. These hydrogels were found to be more swollen at low temperatures.

1.1.1. Synthetic Polymers

Synthetic polymer hydrogels are manufactured from poly(hydroxyethyl methacrylate), poly(ethylene glycol), poly(vinyl alcohol), polyvinylpyrrolidone, polyimide, polyacrylate, polyurethane or their derivatives [9].

The study of super-absorbent, self-crosslinking sodium polyacrylate [10] hydrogel by reversed-phase suspension under gamma-ray irradiation can be given as an example of synthetic hydrogels. Additionally, Sirkecioğlu *et al.* experimented with polyethylene glycol (PEG)/castor oil (CO)-based polyurethane hydrogels using one-shot bulk polymerization methods for biomedical applications [11]. They used hexamethylene diisocyanate as diisocyanate component and 1,4 butane diol as chain extender. Polyurethane hydrogels were prepared in three series: with crosslinker and catalyst, with crosslinker and no catalyst, and with neither crosslinker nor catalyst. They investigated the effect on ratio of CO/PEG, and also the effect on presence of the crosslinker/catalyst on physical and surface properties of polyurethanes.

1.1.2. Natural Polymers

The development and application of biopolymers have been approved owing to their biocompatibility, biodegradability and nontoxicity properties. Collagen/gelatin, chitosan, hyaluronic acid, chondroitin sulfate, alginate, agar/agarose, fibrin are natural polymers used in several biodegradable hydrogel preparations [12].

Patenaude *et al.* functionalized synthetic oligomers and carbohydrate polymers (hyaluronic acid, carboxymethyl cellulose, dextran and methyl cellulose) using hydrazide or aldehyde groups to obtain injectible, mixed natural-synthetic hydrazone-crosslinked hydrogels with various modular properties. Modifying one property selectively and maintaining the others constant provides an adaptable potential method for in vivo applications [13].

Besides, Sadeghi *et al.* synthesized starch-based superabsorbent hydrogel with acrylic acid (AA) and 2-Hydroxy ethyl methacrylate (HEMA) mixtures by graft polymerization [14]. pH responsive hydrogels that are acceptable between pH 2-8 were obtained. The on-off switching behaviour provides the hydrogels to be remarkable candidates for controlled drug delivery.

1.1. Chitosan and Chitosan Based Hydrogels

1.2.1. Definition

Chitosan is a water-insoluble, linear polysaccharide that has randomly distibuted β-1-4 linked D-glucosamine/N-acetyl-D-glucosamine functional groups [15].

Chitosan is soluble in dilute acidic solutions below pH 6. Because it possesses a primary amino group, it can be considered as a strong base with a pKa value of 6.3 [16]. The most common solvent for chitosan is 1% acetic acid of which pH is 4. Also, chitosan is insoluble in many organic solvents, such as dimethylformamide and dimethyl sulfoxide

[17]. Some factors that affects solubility of the polysaccaride are temperature, time of deacetylation, and alkali concentration. During dissolution of chitosan, hydrogen bonds between polymer chains are broken and crystallinity is shown to decrease. That reduced crystallinity is maintained through freeze-drying of the chitosan solution [18].

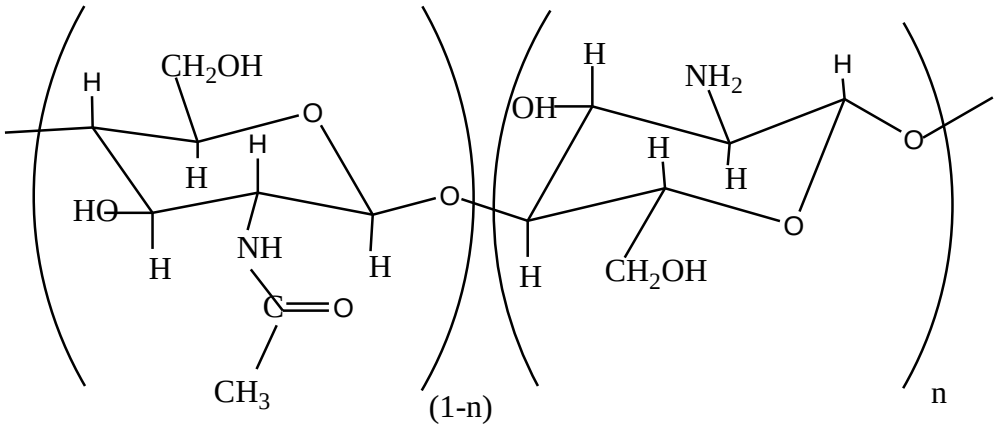

Figure 1.1. Molecular Structure of Chitosan.

It is actually a copolymer that is a partially deacetylated form of chitin; a polymer made up of acetylglucosamine units [19]. Additionally, it is the only known cationic polysaccharide [20].

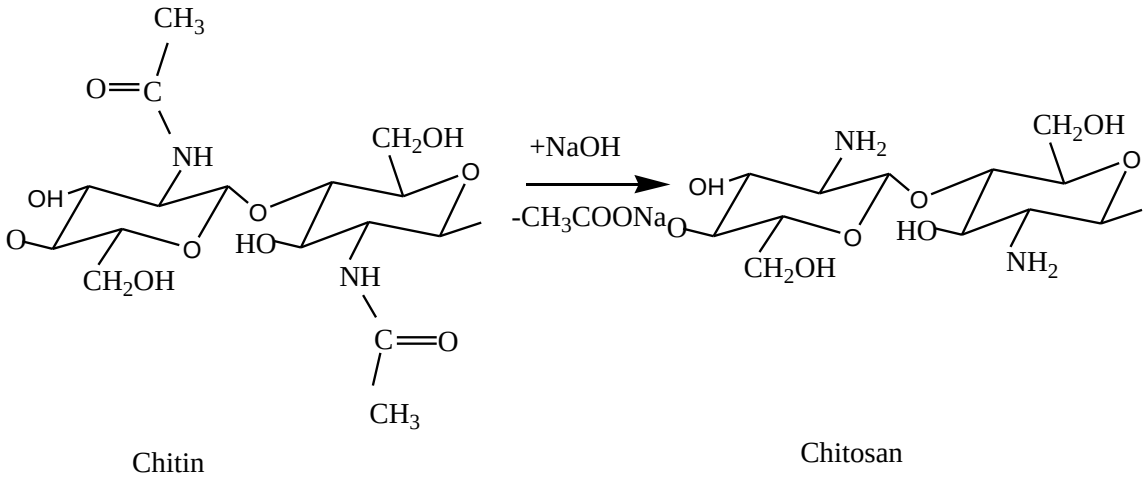

Figure 1.2. Deacetylization Reaction of Chitosan.

1.2.2. Crosslinking of Chitosan

Crosslinking can be beneficial for the resistance of chitosan against acid and alkali solutions, however there will be loss in chain flexibility. As a result, adsorption capacity will decrease. For instance, chitosan beads have higher adsorption capacities than crosslinked chitosan beads but the latter are stable in low pH solutions [21].

In order to crosslink chitosan, bi- or polyfunctional crosslinking agents such as glutaraldehyde [22], epichlorohydrin [23], ethylene glycol diglycidyl ether [24], benzoquinone [25], phosphorous oxychloride ($POCl_3$) [26], carboxylic acids (malic, tartaric, citric, malonic, succinic, glutaric and adipic acid) [27], maleic anhydride, glyoxal or isocyanates are needed. However these crosslinking agents aren't classified as safe or environmentally friendly [21]. Glutaraldehyde is known as neurotoxic and glyoxal is mutagenic [28].

Sodium trimetaphosphate [29], sodium tripolyphosphate [29], genipin [28] and citric acid [27] are known as safe crosslinking agents for their non-toxic properties. These can be used as an alternative for food industrial procedures. Genipin is already being used in herbal medicine industry. Crosslinked hydrogels are more resistant to shear, low temperatures and low pH than neat polysaccharides in their powdered form. In addition, crosslinking can decrease the amount of crystalline domains in the polysaccharide [21].

Chitosan is biodegradable because of the presence of the enzyme, chitosanase [30]. The biocompatible polymer chitin is obtained from the cuticle of the marine crustaceans, such as crabs and shrimps [31]. Chitosan is produced from chitin via removal of the acetyl groups with concentrated aqueous/alcoholic sodium hydroxide solution. Either a nitrogen purge or sodium borohydride solution addition is applied in order to avoid any side reactions [32].

1.2.3. Properties and Applications

Chitosan is a common interest for biomedical and pharmaceutical areas, i.e. artificial skin [31], wound dressing [31], and drug carriers [33]. It also plays the role of a hydrogel material due to its excellent biodegradability, hydrophilicity and selectivity due to its amino and hydroxyl functional groups [34].

Chitosan is a good candidate for supporting gene delivery [35], cell cultures and tissue engineering [36]. The advantage of chitosan for gene transfer, unlike other synthetic polymeric vehicles, is that it is comparably nontoxic. Chitosan/DNA complexes are formed with the help of electrostatic interactions between the primary amino groups and phosphate groups. It is strong enough to resist DNA unpacking within *cells t*. Additionally, when chitosan is planned to be used in drug delivery, pH becomes a crucial factor [37].

Some studies show that chitosan can be modified by attaching to sugars, dendrimers, cylodextrins, crown ethers and glass beads [20]. Chitosan modification is significant because of its solubility in only acidic media and it limits biomedical applications [20]. Several modifications can be conducted by attaching certain functional groups in order to control hydrophobic, cationic and anionic characters. Sugar modified chitosans are widely used in drug delivery systems due to their specific functionality. While modification is being carried out, keeping chitosan water-insoluble would render it disadvantageous in using for antibacterial purposes [38] due to its conditional activity in only acidic medium [39]. The antibacterial activity of chitosan relies heavily on the molecular weight and the degree of deacetylation. Jung *et al.* prepared water soluble chitosan (WSC) derivatives by anionic side chain grafting which contains significant zwitterionic properties. According to their research, water soluble chitosan shows more reactivity than water insoluble chitosan.

In addition, chitosan has the ability to maintain its fundamental skeleton despite the addition of various and compatible functional groups. After modification, researchers continue to add new properties even though chitosan maintains the original physicochemical and biochemical properties.

Chitosan has received the status of GRAS (generally recognized as safe) by the FDA (Food and Drug Administration). However official clearance is needed for use in food formulations [15].

The physical properties of chitosan depend on their molecular weight, degree of deacetylation (DD), sequence of the amido/acetomido groups and the purity of the products [40].

Toxic pollutants should be removed from water through an adsorption method by chitosan. The powder form of chitin and chitosan is used in sorption columns [41]. The benefit of chitosan being an optically active biopolymer and having a strong affinity for transition metals are the reason of usage [18].

Adarsh *et al.* modified chitosan crosslinking with glutaraldehyde to make beads and membranes and the properties of these products were studied [42]. It was concluded that crosslinked chitosan beads have higher adsorption degrees than chitosan flakes and crosslinked chitosan membranes. The maximum adsorption was observed by Chromium (88%), followed by Cadmium, Copper, Nickel, Silver, Lead and Zinc.

Besides transition metal adsorption, chitosan is widely used in dye adsorption applications. The sorption capacity depends on the degree of N-acetylation, molecular weight, solution properties and changes with crystallinity, affinity for water, percent deacetylation and amino group content [43]. Chitosan has a low surface area of $16 m^2 g^{-1}$. Porosity, surface specific area [21] and particle size of sorbents also affect the adsorption efficiency.

Li *et al.* used chemically crosslinked chitosan beads in order to adsorb anionic dyes in aqueous solutions [44]. They prepared these beads by adding the chitosan solution dropwise from a burette to a solution of sodium tripolyphate (TPP) via its ionic crosslinking effect. After this method was carried out, the beads were washed with deionized water and kept in a distilled water solution. A batch system was then prepared to study the adsorption of four reactive dyes, three acid dyes and one direct dye from aqueous solutions. The beads were observed to have an average adsorption capacity of 2200 mg/g at pH 3-4, 30^oC; which is 9 times greater than the commercially activated carbon.

Crosslinked chitosan is insoluble in acidic solution and it is known to have strong mechanical properties.

Adsorption capacity also depends on temperature. A study was conducted by Cestari *et al.* which considered anionic dye adsorption with crosslinked chitosan beads [22]. They investigated the effects of chemical structures and temperature on the adsorption kinetics of the dye. The crosslinked beads were used to adsorb the yellow-, blue- and red- anionic reactive dyes from aqueous solutions at pH 2. It was reported that the adsorption of the yellow-dye increased at temperatures 25^{o}C to 50^{o}C, whereas the adsorption of the blue-dye decreased within the range of 25^{o}C to 50^{o}C. Interestingly, the adsorption of the red-dye decreasing occurred from 25^{o}C to 35^{o}C and from 45^{o}C to 50^{o}C increasing happened. According to Avrami Kinetic Model which was used while evaluating kinetic data, the greatest values of the Avrami parameter n were foumd at the highest values of the temperture.

1.2.4. Chitosan Based Hydrogels

Chitosan is a biocompatible material that can be used in hydrogel preparation for biomedical aims. Ray *et al.* prepared glutaraldehyde crosslinked chitosan-based hydrogel membranes and investigated hemocompatibility, cytocompatibility, mechanical and pH-dependent swelling properties [45]. These hydrogel membranes exhibited higher swelling ratios at lower pH and resulted as highly hemocompatible in the presence of human blood. These selective drug delivery systems can be used in the stomach.

Additionally, Hong *et al.* conducted crosslinkable, water-soluble chitosan derivative at pH 7 and body temperature [46]. They searched in vitro-degradation and chondrocyte-encapculation of these hydrogels. The encapsulated chondrocytes in the chitosan hydrogel survived in the 12-d *in vitro* culture period. Furthermore, the chitosan hydrogel prepared from 10 mM ammonium persulfate/tetramethylethylenediamine was non-degradable even in lysozyme/PBS solution after 18 days. These features provide the chitosan hydrogels injectible scaffold application in othopaedics.

Chemically modified chitosan can be adjusted to the biofabrication of 3-D scaffolds by photopolymerization. Kufelt *et al.* prepared water-soluble photosensitive chitosan hydrogels by crosslinking chitosan with poly(ethylene glycol) diacrylate [47]. *In vitro* studies resulted that modified chitosan is biocompatible and can be used in tissue engineering.

Mahdavinia *et al.* prepared chitosan-poly(sodium acrylate-co-acrylamide) hydrogel hybrids owing to the reaction of alkoxide anions in chitosan and nitrile groups of poly(acrylonitrile) (PAN) and studied swelling properties of these hydrogels [48]. The hydrogels having 60 wt% of PAN resulted equilibrium-swelling ratio as 262 g/g for water.

1.3. Hydrogel Composites

Hydrogels are impotent to resist mechanical strength or wear abrasion. Nanosized reinforcements that contain strong interfacial interactions with considerable strength have been recently recognized as advantageous when trying to improve both biological responses and mechanical properties. Some examples of these reinforcing agents include hydroxyapatite [49], nanoclay [50], carbon nanotubes [51] (CNTs), titanium dioxide [52], graphene [53], silver and gold [54].

When clays in their original form or organo-modified clays are added into the hydrogel formulation, new generation of hydrogels takes place creating hydrogel composites & hydrogel nanocomposites.

Natural aluminasilicate inorganic compounds are typically used in hydrogel composites and nanocomposites because of their abundance, low price and hydrophilic nature. They offer improved thermal, mechanical, optical and electrical properties compared to their sole polymer matrix. Clay type and content affects swelling capacity, swelling rate and reswellability [3].

Vymazalova *et al.* carried out silicone-rubber hydrogel composites with lightly crosslinked powdery polymers of 2-hydroxy ethyl methacrylate (HEMA), acrylamide (AA)

or their copolymers with methacrylic acid (MAA) as a hydrogel base and examined these in terms of scanning electron microscope (SEM) via fracture surfaces of the materials [55]. These hydrogel composites resulted that could be inserted into a body cavity in terms of medical applications.

Chang *et al.* prepared gelatin[GEL]-hydroxyapatite[HAp] nanocomposites for biomimetic applications by precipitating hydroxyapatite nanocrystals in an aqueous solution of gelatin [56]. The chemical bonding between carboxyl ions of gelatin molecules and calcium ions of HAp nanocrystals were observed in FTIR analysis.

1.3.1. Chitosan Hydrogel Composites

Biodegradability, hydrophilicity and selectivity features of chitosan has regained attention in recent years and has found a place in composite applications. Thein-Han *et al.* fabricated high (400 kDa) and medium (250 kDa) molecular weight chitosan scaffolds with 0.5, 1 and 2 wt% of nanohydroxyapatite (nHA) by freezeing and then lyophilizing methods [49]. In chitosan-nHA composite scaffolds cell proliferation was 1.5 times greater than pure chitosan and observed through qualitative analysis of fluorescence microscopy. The pore size and porosity are crucial for the growth of these cells. These scaffolds are potential bone regenerating materials.

Jirandehi *et al.* prepared chitosan-based hydrogel nanocomposites in presence of MMT-Na^+ nanoclay to study controlled release of cisplatin drug between pHs 1-12 and at 7.4 [57]. The swelling tests showed that the water absorption rate is higher in acidic medium. Govindan *et al.* synthesized Silver nanoparticles by chemical reduction and prepared 20wt% containing chitosan nanocomposites which showed good antimicrobial and antitumor properties [58].

1.4. Halloysite, Its Properties and Use as Reinforcer in Hydrogels

Halloysite is a clay mineral that has a chemical formula of $Al_2Si_2O_5(OH)_4.nH_2O$. This dioctahedral 1:1 clay mineral is accessible in soils, particularly in wet tropical and

subtropical regions [23]. There are also halloysite reserves in the Turplu Area, Balıkesir, Turkey [59].

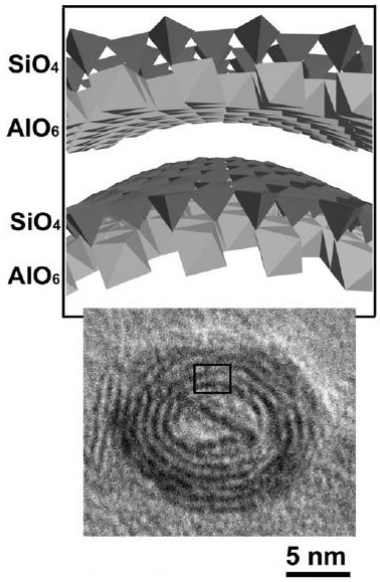

Figure 1.3. Schematic drawings showing the multi-walled structure of nanotubes as a combination of AlO_6 octahedral with SiO_4 tetrahedral [60].

HNTs are composed of double layers of aluminum, silicon, hydrogen. They have ultra-tiny hollow tubes with diameters smaller than 100 nanometers and with lengths ranging from 500 nanometers to 1.2 microns. Outer surfaces contain SiO_2 that have a negative charge (zeta potential) at pH 6-7, whereas the inner cylinder core has a slightly positive charge which is similar to Al_2O_3 [61]. The positive charge of the inner lumen results from the loading negative molecules within emptiness, however, there is a possibility that the negative molecules can be repelled from the outer surfaces at the same time.

HNTs have two types of models: Single-walled and multi-walled [61]. An interesting feature is the cylindrical shape of halloysite nanotubes and its natural reoccurrance in nature [62]. Bi- layered alignment is the main reason due to that two-layered alignment of the tetrahedral sheet of silica is bonded to the octahedral sheet of alumina [63]. The halloysite functions as a polyvalent ion due to the inner and outer lumens containing a net negative charge from the isomorphous substitutions of Al^{3+} for Si^{4+}. This feature makes it a suitable candidate for drug loading [62].

Halloysite can be an alternative for carbon nanotubes (CNTs). HNTs are cheap, abundantly available, environmentally friendly, mechanically strong and biocompatible [23]. It is a unique example of "green" inorganic reinforcing material for polymer [64].

HNTs are advantageous in maintaining uniform nanocomposites which are capable of loading multiple active agents simultaneously [62]. They also have a high aspect ratio, high porosity, no swelling and regeneration ability [65].

Furthermore, Silva et. al reported the anti-inflammatory, cytotoxic and anti-oxidant activity of halloysite by using a series of biological tests [65].

There are several researchers that have studied halloysite containing hydrogels. Halloysite reinforced thermo responsive hydrogels are studied because of their controlled release properties [66]. Lin *et al.* prepared halloysite nanotube composited hydrogels by copolymerization of N-isopropylacrylamide (NIPAM) with silane modified nanotubes through thermally initiated free radical polymerization. The prepared samples were swollen at temperatures below the lower critical solution temperature (LCST). This causes drug release from the lumens of nanotubes. On the other hand, at above LCST, the hydrogel shrinks and the drug release stops.

Another group prepared hydrogel nanocomposites through emulsion polymerization [63] with linear low density polyethylene, acrylic acid and two types of clays: Kaolinite and Halloysite. Irani *et al.* found that their hydrogel composites have are more porous and have a higher swelling ratio than clay-free hydrogels. The hydrogel containing kaolin had a higher water absorbency than the hydrogel composites containing halloysite.

Tu *et al.* prepared nanocomposite hydrogels with halloysite, oligo(trimethylene carbonate)-poly(ethylene glycol)- oligo(trimethylene carbonate)- diacrylate (TPT) and alginate sodium (AG) [67]. The addition of small amounts of halloysite (2 wt%) improved the mechanical properties of the hydrogel.

Some research groups focused on modification of halloysite. Pal *et al.* explored the effects of halloysite nanotubes (HNTs) and modified halloysite nanotubes (M-HNTs) to be used in blend systems of polar polyoxymethylene (POM) and nonpolar polypropylene (PP) [68]. They modified halloysite with N-(β-aminoethyl)-γ-aminopropyltrimethoxysilane (APTMS). M-HNT behaves like a reinforcing agent in polar-nonpolar hybrid system. Using properties better than the pure blend system.

Yuan *et al.* tried surface modification of halloysite with γ-aminopropyltriethoxysilane (APTES) to demonstrate the effects on loading and releasing of a model dye [69]. The dye loading was 32% higher than the unmodified version and the release was prolonged compared to that of the unmodified one. Dye release was also prolonged for those with a lower pH value. For instance, dye release for pH 10 lasted three times as much than for pH 3.5.

Besides adsorption studies some research groups focused on the desorption features of halloysite. Chen *et al.* studied the recovery of halloysite from two anionic azo dyes: Methyl Orange (MO) and Congo Red (CR) [70]. They found that the adsorbed methyl orange is removed completely by deionized water. In contrast, congo red desorption is difficult to remove in strong acidic and alkaline environments. Another group, Peng *et al.* found that desorption of methylene blue from chitosan-halloysite composite hydrogel beads can be achieved by a NaOH solution and acetone [34]. They also studied the same process with the malachite green dye but the results were proven unsuccessful.

There has been multiple studies dedicated to the unfolding of the tubular structure of halloysite. Tang *et al.* changed the period of phenylphosphonic acid (PPA) treatment with halloysite and observed different levels of enfoldment and intercalation [71]. Increasing intercalation of halloysite also increased fracture toughness of composites. Formation of micro-cracks and plastic deformations in the interfaces occurred when the halloysite was treated with acid. The contact area between halloysite and epoxy also increased and its morphology changed from nanotubes into nanoplatelets.

Lvov *et al.* reported an essential increase of halloysite lumen diameter by selective etching of alumina sheets within its lumen while also performing its kinetic analysis of

lumen etching at various temperatures were performed [72]. However, due to decrease of wall thickness, it was found that acid treatment on halloysites in polymer composites reduces the mechanical properties, such as bending stiffness and tensile strength.

1.5. Chitosan-Halloysite Studies

In the literature there are some studies concerning the chemically crosslinked structure with epichlorohydrin. It was reported that novel hybrid hydrogels can be prepared from chitin NaOH/urea aqueous solution containing halloysite nanotubes by crosslinking with epichlorohydrin [23]. Although the compressive strength and shear modulus of chitin increased with halloysite addition, the swelling ratio decreased. Also hybrid hydrogels had more malachite green (cationic dye) absorption capacity than neat chitin hydrogel. Highly porous structures were observed in the hybrid hydrogels via scanning electron microscopy (SEM).

Besides making hydrogels, Liu *et al.* studied chitosan-halloysite nanotubes bionanocomposites via solution casting and investigated their structure, mechanical properties and biocompatibility [73]. They confirmed electrostatic attraction and hydrogen bonding interactions. Addition of halloysite enhanced the tensile strength and Young's modulus. Also, the storage modulus and glass transition temperature of the films increased.

Blending with halloysite changes surface nanotopography and increases roughness of chitosan films. In vitro fibroblasts prove that the nanocomposite films are cytocompatible even when the halloysite content is 10%. At the end, chitosan/HNTs nanocomposite films turn out to be potential scaffold materials for tissue engineering.

Another study about chitosan-halloysite nanocomposite scaffolds were conducted by Liu *et al.* for tissue engineering [74]. The method of this study was the combination of solution mixing and freeze-drying techniques. Compressive strength, compressive modulus and thermal stability were enhanced in nanocomposite scaffolds when compared with neat chitosan scaffolds. The swelling, however, was shown to have decreased. These nanocomposites were cytocompatible, even when halloysite content was 80%. The study

was particularly intrested in the different properties that could be altered using the freeze drying technique; such as microstructure, cyrstallinity and mechanical strength.

Recently, the same research group prepared composite hydrogel beads with chitosan and halloysite by the dropwise addition and pH precipitation method [34]. Halloysite influence on the appearance, diameter, microstructures, thermal stability were characterized. Dye adsorption properties of the beads and fundamental adsorption behaviour were studied. Both the cationic methylene blue and malachite green were chosen as model dyes.

Although very recently a study was published on chemically crosslinked chitosan-halloysite hybrid hydrogels, a systematic and detailed investigation on the preparation and characterization of and fully natural physically crosslinked hydrogel nanocomposites having both components has not yet been conducted.

2. AIM OF THE STUDY

In today's world within the effect of technological development and industrial manufacturing, the society has some environmental problems. The sources of earth are getting depleted and the ones that aren't used yet, they are being polluted. One of those sources is water and we wanted to achieve the design and production of a multifunctional/multicomponent material for waste-water treatment.

In recent years polymeric nanocomposites gained high attention due to their superior mechanical, thermal and adsorption capacities as compared to neat polymers and micro-composites. Therefore the main objective of this study was to prepare and characterize a hydrogel nanocomposite which has high water absorption ability, selectivity towards pollutants, high dimensional and mechanical strength as well as biocompatibility.

Special attention was paid to design and synthesis of the hydrogel nanocomposites by choosing appropriate biopolymer and reinforcer which are suitable for stiffening/toughening and dye adsorption. For this purpose halloysite nanotubes (HNTs) and chitosan were chosen as main components. There is a need for naturally available, cheap, light, mechanically strong and biocompatible nanoparticles while preparing chitosan nanocomposites and it leads us to halloysite nanotubes (HNTs), naturally occurring silica nanotubes, having large surface area and pore volume, tunable mesopore size and biocompatibility. It has been thought that both reinforcing and dye adsorption performances of Halloysite could be improved via non-chemical expansion of its lumens.

The resultant nanocomposite hydrogels were characterized in terms of structure , wet mechanical strength, water absorption and dye adsorption properties by making use of Testing Methods and Swelling and Dye Adsorption Properties and Fourier Transform Infrared Spectroscopy (FTIR), Scanning Electron Microscopy (SEM) and Thermal Gravimetric Analysis (TGA) were all conducted.

3. EXPERIMENTAL

3.1. Materials

Chitosan powder (Figure 1.1) was purchased from Sigma Aldrich International Inc. and used without further purification. Its degree of deacetylation (DD) and molecular weight are 75-85 % and 50,000-190,000 Da based on viscosity. Purified HNTs whose structures are given in Figure 1.3 (Tabanköy-Balıkesir, Turkey) are kindly supplied from ESAN-Turkey. Deionized water from Milli-Q water system was used to prepare the aqueous solutions of 1 % Acetic Acid, 1 M NaOH and dye solutions of Nile Blue (NB) and Bromocresol Green (BCG) with the analytical grade $1x10^{-5}$ M.

3.2. Expansion of Halloysite Nanotubes

Halloysite nanotubes are proceeded through solution by mixing of HNTs in deionized water, freezing and subsequent drying with lyophilizing method. The typical procedure is as described below. 1 g of HNTs is dispersed in 20 ml of water at 50 ° C for 2 hours and then the solution was cooled to -22 °C overnight in a freezer and then dried via lyophilization at -45 °C using a Labconco FreeZone 1 Liter Benchtop Freeze-Dry System.

3.3. Synthesis of Neat Chitosan and Chitosan-Halloysite Composite Hydrogels

The chitosan and chitosan-HNTs nanocomposite hydrogels were prepared by solution mixing and subsequent freeze-drying method as described below. Calculated amount of HNTs were dispersed in 10 ml of 1 % acetic acid solution, mixed for 6 hours at 750 rpm using Heidolph MR Hei Standard. Then 0.1 g of chitosan was added to the halloysite solution. Mixture was continously stirred overnight and poured into a cylindirical polystyrene mould with 30 mm diameter and 10 mm height . Subsequently it

was frozen at -20 °C overnight in a freezer and then freeze-dried at -45 °C . For comparison, neat chitosan hydrogels were also prapered in the same way but without addition of HNTs. After lyophilization all hydrogels were put into the 1 M NaOH solution to remove excess acid for 1 hour, then rinsed with deionized water and . held in deionized water for 24 h by changing deionized water 2-3 times. Stable form of hydrogels were frozen and lyophilized as described above. The hydrogels were named as HLyCH and XPHLyCH where y indicates halloysite (HL) and cryo-expanded halloysite (XPHL) percentages in total amount of chitosan (CH) hydrogels.

3.4. Characterization Techniques of Hydrogel Nanocomposites

The BET isotherms were obtained at liquid nitrogen temperature 77 K by using Quantachrome Nova 2200e automated gas adsorption system. The specific surface areas were determined using multi-point BET analysis and the pores sizes were measured by the BJH method of adsorption.

X-ray diffraction (XRD) measurements of halloysite nanotubes as well as dried hydrogels were conducted on a Rigaku D/Max 2200 Ultimat diffractometer (Rigaku, Tokyo, Japan) with CuKα radiation (λ=1.54°A), operating at 40 kVand 40 mA with a scanning rate of 2°/min.

Fourier transform infrared (FTIR) spectra of nanocomposite hydrogels were obtained with a Thermo Scientific Nicolet 380 FTIR Spectrometer with a diamond ATR accessory. The result was evaluated by EZ Omnic.

SEM analyses of the nanotubes and freeze-dried hydrogels were carried out by using ESEM-FEG/EDAX Philips XL-30 (Philips, Eindhoven, The Netherlands) within accelerating voltage of 5 kV. Before SEM observation, the freeze-dried hydrogels were sectioned and were sputter coated with platinum using a sputter coater.

TEM analysis was performed using a JEOL 2000FX (JEOL, Tokyo, JAPAN) TEM instrument operating at an acceleration voltage of 200 kV. The particles were transferred onto carbon support films on 300 mesh copper grids.

Swelling behaviour of the hydrogels was followed by gravimetric measurements. The freze-dried polymeric samples were weighed and immersed in deionized water and taken out at regular intervals to measure change in weight. Water uptake with respect to time was obtained by periodically removing the samples from water quickly drying, and reweighing.

The measurements were conducted at 25 °C in a water bath. The percent swelling (water uptake) was calculated with the following equation:

$$S\,\% = \frac{m_t - m_0}{m_0} x100 \qquad (3.1)$$

where m_t is the mass of the swollen gel at time t and m_0 is the mass of the dry gel.

The wet mechanical strengths of the hydrogels were measured by performing uniaxial compression experiment with a Zwick/Roell Z1.0 Universal Testing Machine (Zwick GmbH & Co.KG, Germany) equipped with a 50 N load cell and the data was analyzed using Zwick/Roell testXpert II software. All the mechanical measurements were performed on the wet samples at room temperature and at a compression rate of 2 mm/min. Before the analysis, the hydrogels were immersed in water upto equilibrium swelling. The measurements were conducted until a displacement of 80% of the examined sample was reached. The compression modulus was calculated from the slope of the initial linear region of stress-strain curve. Tougness was calculated as work up to maximum force of the stress-strain curves. Compression strength at the maximum strain was obtained from the original output of the instrument.

Ultraviolet-Visible analysis (UV-Vis) was performed on Shimadzu Spectrophotometer UV-120-01 under the wavelenths of 616 nm for BCG (Figure 3.2) and 635 nm for NB (Figure 3.1).

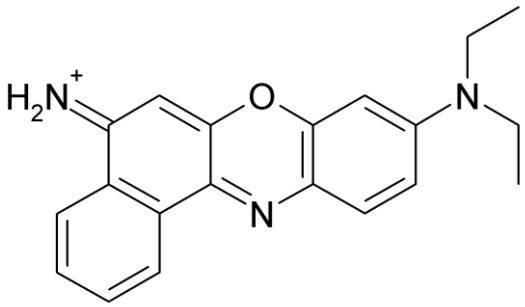

Figure 3.1. Molecular Structure of NB.

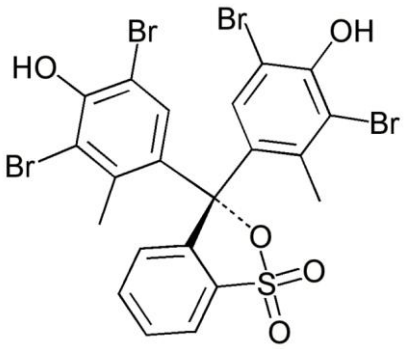

Figure 3.2. Molecular Structure of BCG.

Removal of the cationic dye (Nile Blue) and the anionic dye (Bromocresol Green) from the solution was studied by using different beakers containing 100 ml of $1x10^{-5}$ M dye solutions and the amount adsorbed on the hydrogel was calculated by the following equation:

$$q = \frac{(c_0 - c_t)v}{w} \qquad (3.4)$$

where q is the amount of the dye adsorbed onto the unit amount of the hydrogel (mg/g), c_0 was the initial concentration of dye (mg/L), c_i was the final or equilibrium concentration of dye (mg/L), V was the volumeof the dye solution (L) and W was the weight of the hydrogel (g). At desired time intervals, the remaining amount of dye in the aqueous solution was determined by UV spectrophotometry by monitoring the absorbance value.

Desorption was conducted with 0.1 L of 0.5 M NaOH aqueous solution. Hyrogels that adsorbed anionic or cationic dyes were kept in NaOH solution for 24 hours. After 24 hours, they were removed and washed with deionized water for 3 times in another 24 hours

and then placed in -20 ℃ freezer and lyophilized finally. Second dye adsorption test was applied onto those hydrogels to search for reusability.

4. RESULTS AND DISCUSSION

4.1. Expansion of Halloysite

4.1.1. Morphological Characterization

Morphologies of the original (HL) and expanded form of halloysite (XPHL) are given in Figure 4.1 and Figure 4.2.

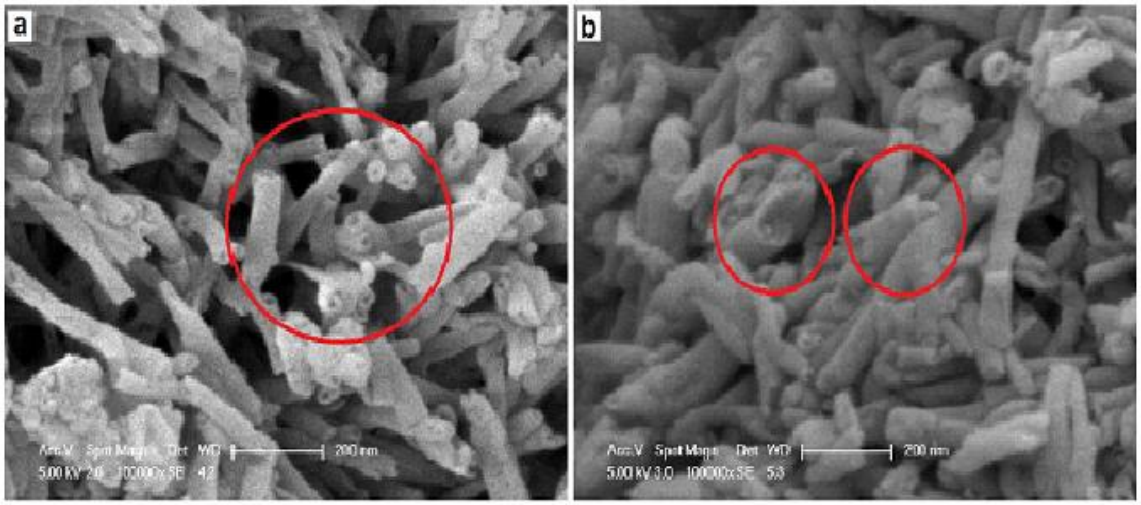

Figure 4.1. SEM images of (a) original Halloysite and (b) expanded form of Halloysite.

Pure halloysite is a white fine powder having a tubular structure with external diameters of 40-50 nm and lumen sizes of 10-20 nm. The length of the tubes is between 0.5-1.5 μ. The expansion of the tubular diameters can be easily observed (Figure 4.1b circled area).

Nanotubes swell with water and then they are frozen to -20^{o}C subsequently. It is obvious that the process resulted with an increase and enlargement of nanotubes (solid circle). The external diameters increase up to 90-100 nm and lumen sizes reach to 40-50 nm. Some of enlarged nanotubes have shown telescopic extension.

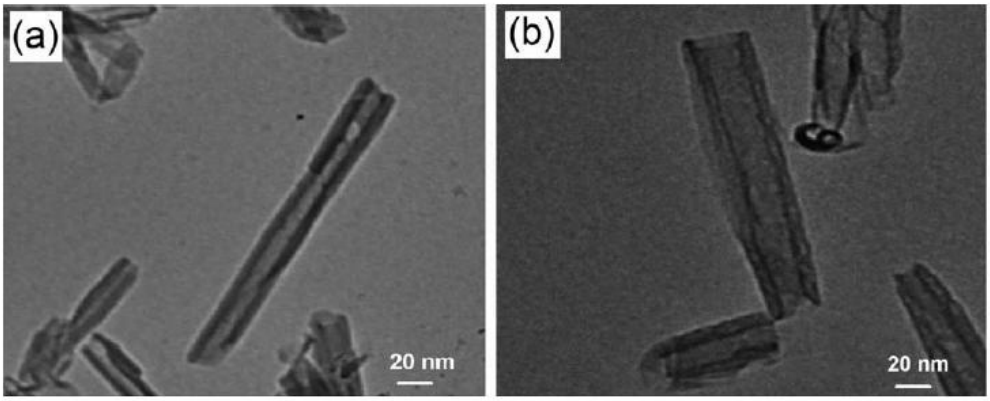

Figure 4.2. High magnification images of Halloysite a) before and b) after cryo-expansion.

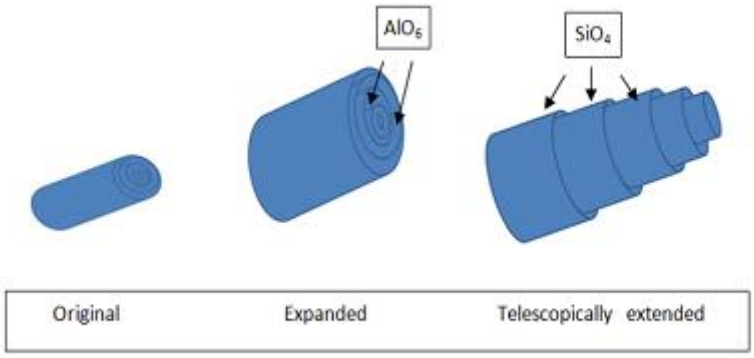

Figure 4.3. Schematic drawings showing the multi-walled structure of nanotubes as a combination of AlO_6 octahedral with SiO_4 tetrahedral as insert and possible morphologies of the nanotubes after cryo-expansion.

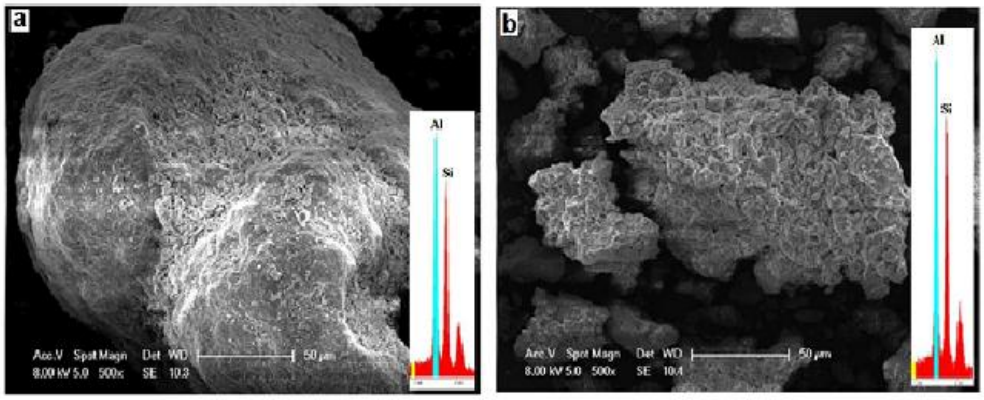

Figure 4.4. ESEM images with accompanying representative EDX spectra from multiple areas on (a) original halloysite and (b) cryo-expanded halloysite.

Rod-like tubular structures and wall thicknesses are preserved as confirmed by further EDX analyses. According to Figure 4.3, both original (HL) and cryo-expanded one (XPHL) are rich with aluminum and silicon. The outer surface of halloysite contains SiO_4 tetrahedral with negative charge, however the inner surface contains octahedral Al-OH functionalities with positive charge [61]. After cryo-expansion, average relative amounts of aluminum increases from 0,30 to 0,32 and for silicon it goes from 0,325 to 0,34. This result indicates that both enlargement and telescopic extension of inner layers occur by putting more extra available Al sites than extra Si sites.

4.1.2. Structural Characterization

In Figure 4.4, X-ray diffraction patterns are shown for original halloysite (HL) and cryo-expanded halloysite (XPHL).

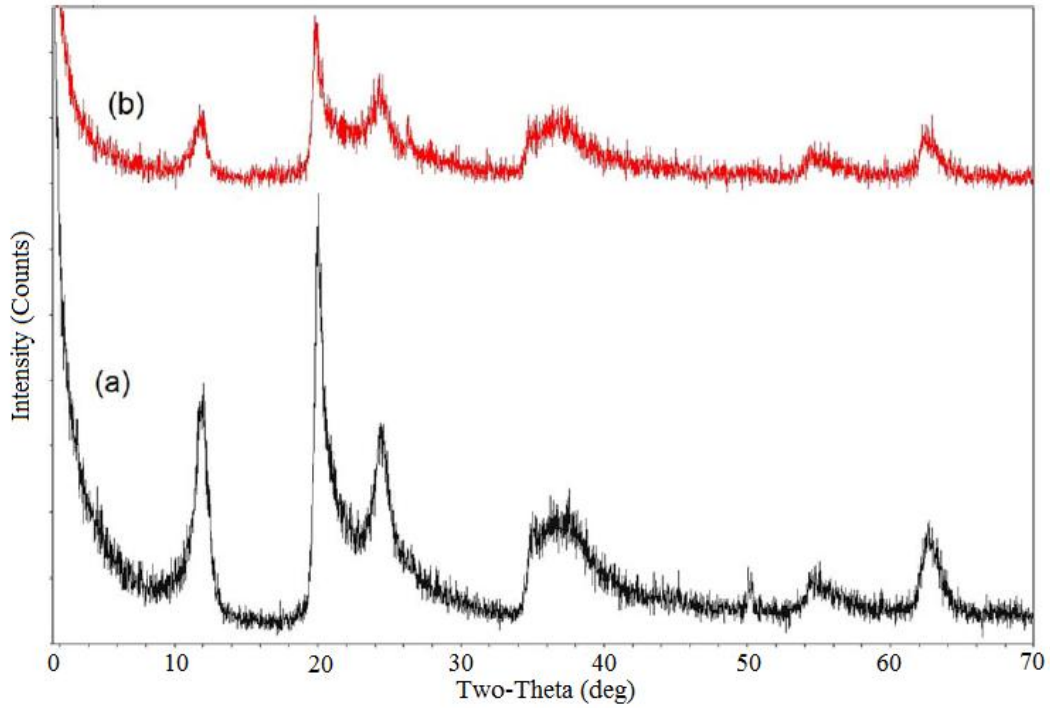

Figure 4.5. XRD patterns for (a) original halloysite (HL) and (b) cryo-expanded halloysite (XPHL).

The original halloysite has 3 main diffraction peaks of 12.24^o indicating (001) basal spacing of 0.719 nm. (002) basal reflection at 24.48^o equivalent to 3.68 Å indicates the dehydrated state. Another diffraction peak (006) of 62.38^o equivalent to 1.467 Å indicates

the nano-tubular structure of halloysite [75]. All angles are written with respect to 2theta. There is a shift of d_{001} reflection towards lower angles and the relative intensity decreases most probably due to the layer space increasing via cryo-expansion and partial loss of the crystallinity in the tube walls [72]. Our results confirms that expansion in nanotubes was successful as a result of the pressure exerted by enlarged ice crystals during lyophilization process. In addition to this, the diffraction peak at 62.38^{o} still exists and shifts to lower angle after lyophilization process. It indicates the preservation of characteristic nano-tubular structure of hallosite with a larger diameter.

The result of N_2 adsorption data agrees on the cryo-expansion of halloysite morphology. In the figure No, isotherms of N_2 adsorption on the surface of halloysite nanotube before and after expansion can be seen.

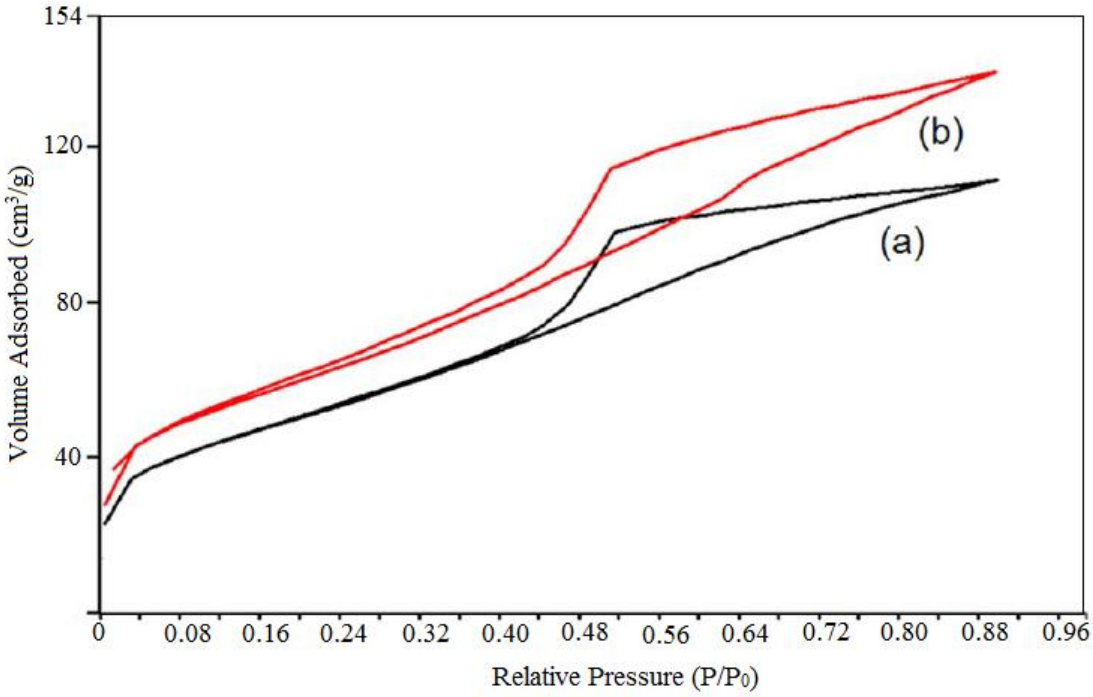

Figure 4.6. Nitrogen adsorption-desorption isotherms of (a) original and (b) expanded halloysite nanotubes.

Both of them reveal Type IV isotherms with hysteresis loops, characteristic of mesoporous materials [76]. The initial parts of the isotherms (at low P/P_0) are associated with monolayer-multilayer adsorption on the surfaces of the halloysite nanotubes. At higher P/P_0 values, capillary condenstaion takes place within pores. There is an increase in

pore volume of the XPHL that also results in higher surface area than HL. Both the expansion of lumens of halloysite and telescopic extension of the inner layers can be deduced from BET, the SEM images and EDX data of HL and XPHL nanotubes. The increase in surface area is related to availability of more adsorption sites and it is expected to help chitosan molecules in interaction with nanotubes to adsorp/diffuse of more water/dye molecules into the hydrogel.

Table 4.1. Surface areas (BET) and total pore volumes (V_{pore}) of Halloysites.

Samples	BET (m^2/g)	V_{pore} (cm^3/g)
HL	54.78	0.087
XPHL	59.25	0.095

4.2. Characterization of Nanocomposite Hydrogels

4.2.1. Chitosan-Halloysite Interactions

FTIR spectroscopy was used to examine the interactions between halloysite and chitosan nanocomposite hydrogels. Spectra are given in Figure 4.6 and Figure 4.7.

1405 cm^{-1} is the characteristic peak for the deformation vibration of the protonated amine group ($-NH_3^+$) and hydroxyl group [73]. The peaks for the chitosan-halloysite nanocomposite hydrogels shift to lower frequencies owing to H-bonding interaction and the electrostatic interactions between halloysite and chitosan in HLCH and XPHLCH hydrogels.

It can be safely concluded that the expected and spectroscopically verified interactions between the components exist.

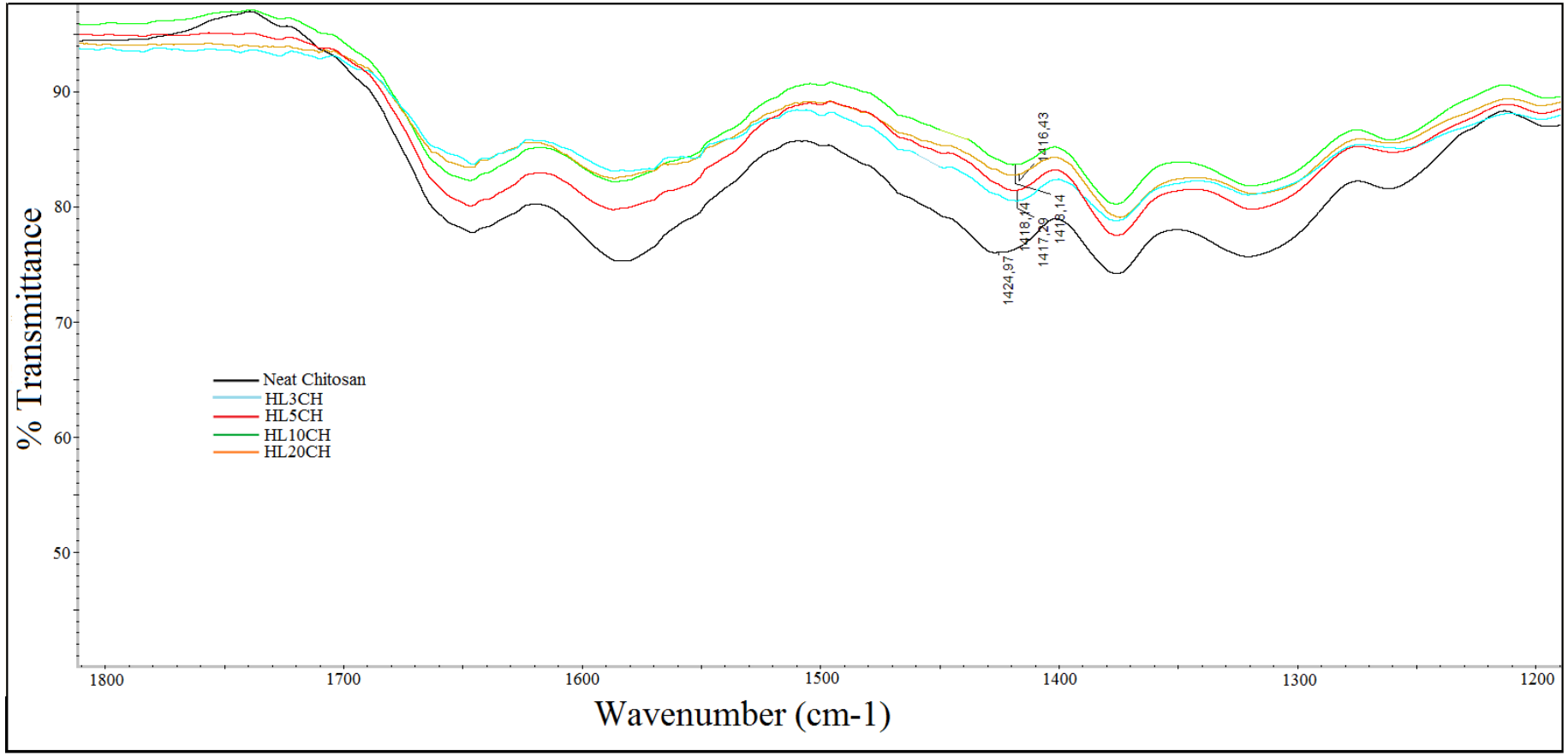

Figure 4.7. Fourier Transform Infrared Spectroscopy of neat chitosan and halloysite (HL) nanocomposite hydrogels.

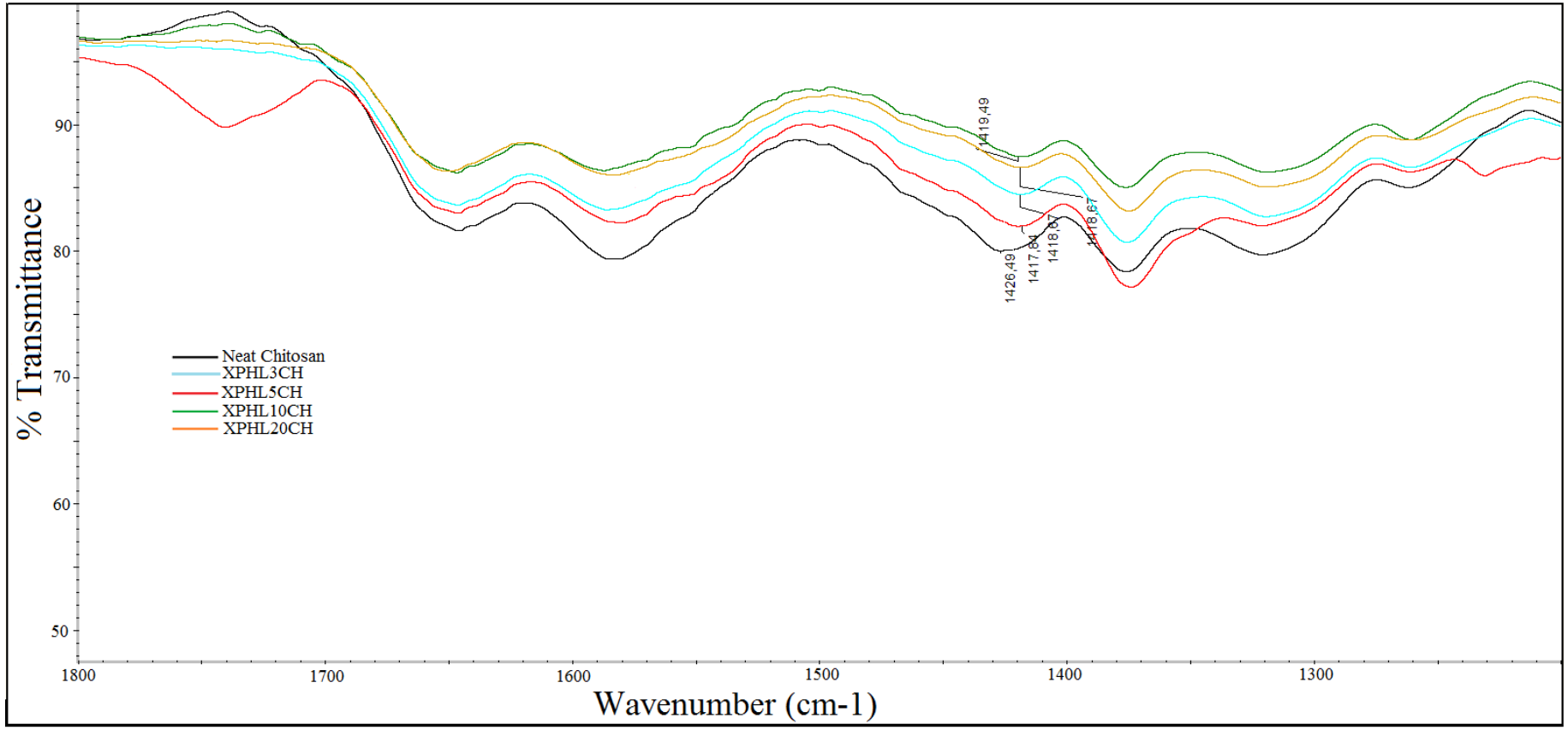

Figure 4.8. Fourier Transform Infrared Spectroscopy of neat chitosan and cryo-expanded halloysite (XPHL) nanocomposite hydrogels.

4.3. Morphology of Chitosan Halloysite Nanocomposite Hydrogels

Figures 4.8, 4.9 and 4.10 show the interior morphologies of neat, HLCH and XPHLCH hydrogels, respectively. All of the hydrogels which are chitosan and its composite forms containing original or cryo-expanded halloysite nanotubes in different amounts showed two-three dimensional porous structures.

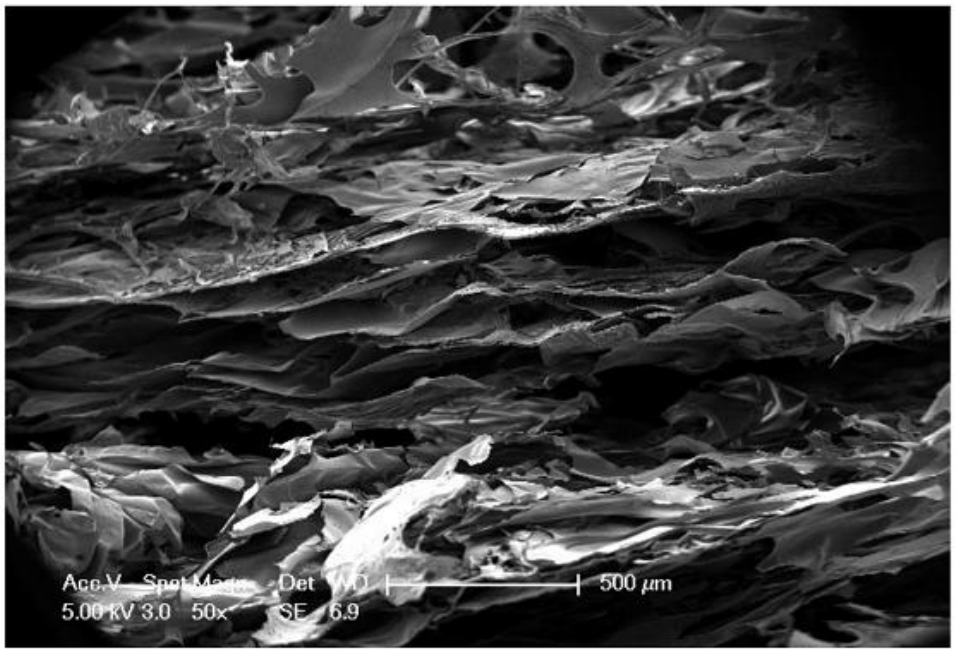

Figure 4.9. SEM image of neat chitosan hydrogel.

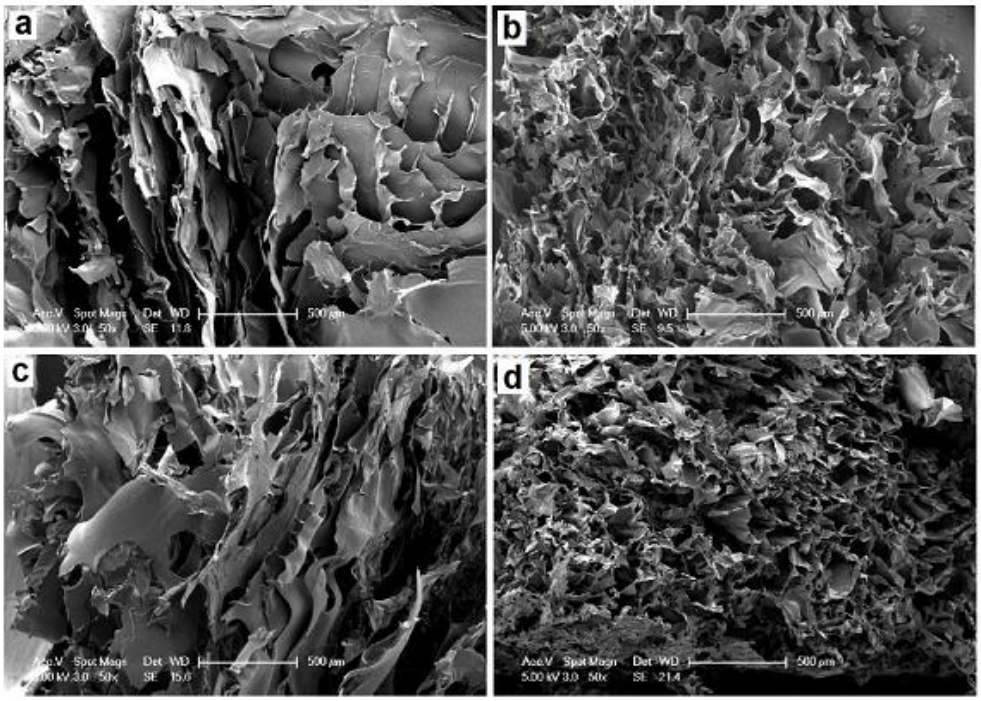

Figure 4.10. SEM images of (a) HL3CH, (b) HL5CH, (c) HL10CH and (d) HL20CH hydrogels.

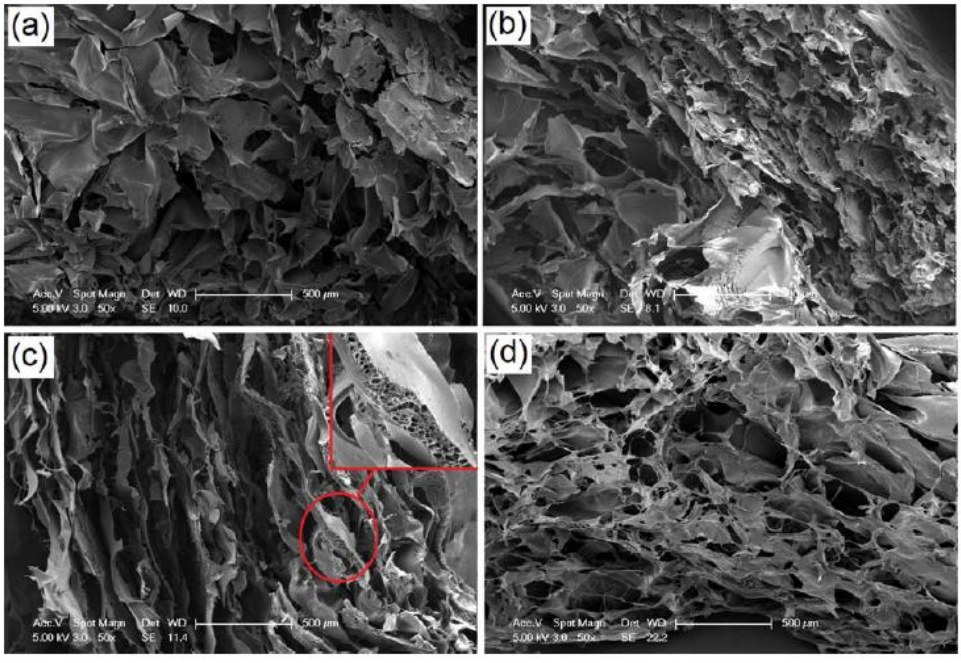

Figure 4.11. SEM images of (a) XPHL3CH, (b) XPHL5CH, (c) XPHL10CH and (d) XPHL20CH hydrogels.

The pores in neat chitosan hydrogels (Figure 4.8) are in irregular-channel shape having a dimension of 20-300 microns resulting from ice segregation induced self-assembly [77]. However, in the composite hydrogels these channels becomes open cells. In the XPHL loaded composite hydrogels, these open cells are distributed in an extended uniform manner having an 50-100 μm range (Figure 4.10).

Zigzag structures and three dimensional orientations of halloysite occur due to intertubular interactions between halloysites and matrix and because of edge-to-edge and face-to-edge interaction between halloysites inside the nanocomposites [78]. The open cell morphology can be an indication of the compatibility between chitosan and halloysite via hydrogen bonding and ionic interactions. Additionally, three dimensional network structure results from the nanosize particle directed assembly. The amount of these open cell morphologies increase up to 5 % loading. Above that percentage, the addition helps to form original chitosan structure again. Both cryo-expansion or telescopic extension of layers having an increase in ionic sites interact with positively charged chitosan to a greater extent and it leads to a better dispersion at early compositions such as 3 % XPHL loading (Figure 4.10a). The nanotube dispersion is better in expanded versions (Figure 4.10), however, in further loadings after 3 %, this expanded/extended tubes have an extra edge hydroxides and it leads to a higher interaction as well as aggregation which results the original irregular channel like morphology. Moreover, some sub-networks occur at cell walls when higher loading of XPHL is conducted (Figure 4.11).

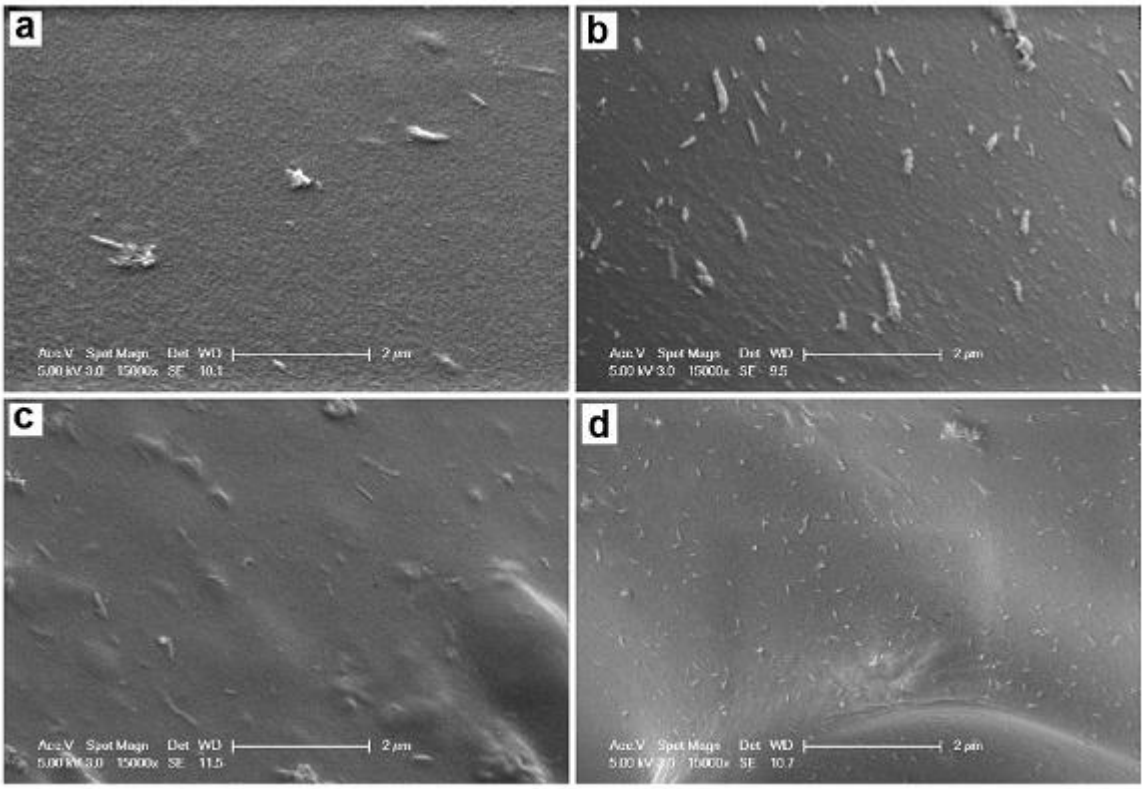

Figure 4.12. High magnification SEM images of (a) HL5CH, (b) XPHL5CH, (c) HL10CH and (d) XPHL10CH hybrid hydrogels.

4.4. Water Absorption Capacity of Chitosan-Halloysite Nanocomposite Hydrogels

The water absorption capacities of neat chitosan hydrogel and the nanocomposite hydrogels with different amounts of HL and XPHL were determined by following their swelling behaviour in water. Swelling plots are given in Figure 4.12 and 4.13.

It is obvious that swelling increases with time up to a certain level and then levels off and indicates the equilibrium between swelling and deswelling.

Although the slope of the curves reaches the equilibrium swollen state within 254 minutes for chitosan hydrogel, HL loaded nanocomposites result faster water absorption within first 60 minutes. However, the water absorption slows down for the composite having cryo-expanded HL because of the enhanced hydrophilic open cell morphology attending as host for water molecules.

Figure 4.12 denote that the maximum attainable swelling in neat chitosan hydrogel is 1750 % while the values for HL and XPHL reinforced hydrogels increases up to 2600 % and 3300 % in a relative manner. The addition of HL into the chitosan hydrogels arrange nano-size directed/ordered morhology with additional open cells and suitable lumens for water molecules. On the other hand, at above 5 % loading of HL swelling decreases to a lower value because of both the high amount of hydrogen bonding between amine, acetamide or hydroxyl groups of chitosan molecules and Si-O groups on the outer surfaces of the nanotubes and ionic interactions between the positively charged chitosan molecules and the negatively charged outer surfaces of halloysite. These type of non-covalent/ionic interactions increases the distinct crosslink density and it leads to less diffusion of water and less swelling of the hydrogel [67]. Besides, partial agglomeration of the nanotubes at higher loadings that was observed in SEM images, might affect the deacrese in water absorption capacity.

While the maximum swelling occurs at 5 % HL loading, this value changes to 3 % loading for expanded halloysite (XPHL) containing composite hydrogels due to cryo-expansion effect. The expansion of halloysite contributes in water absorption of chitosan composite hydrogels at 3 % XPHL loading then their swelling values decrease (Figure 4.13). If the amount of XPHL loading outreaches 3 %, the extra charged surface produced by cryo-expansion induces excess crosslinking and agglomeration and this leads to less swelling.

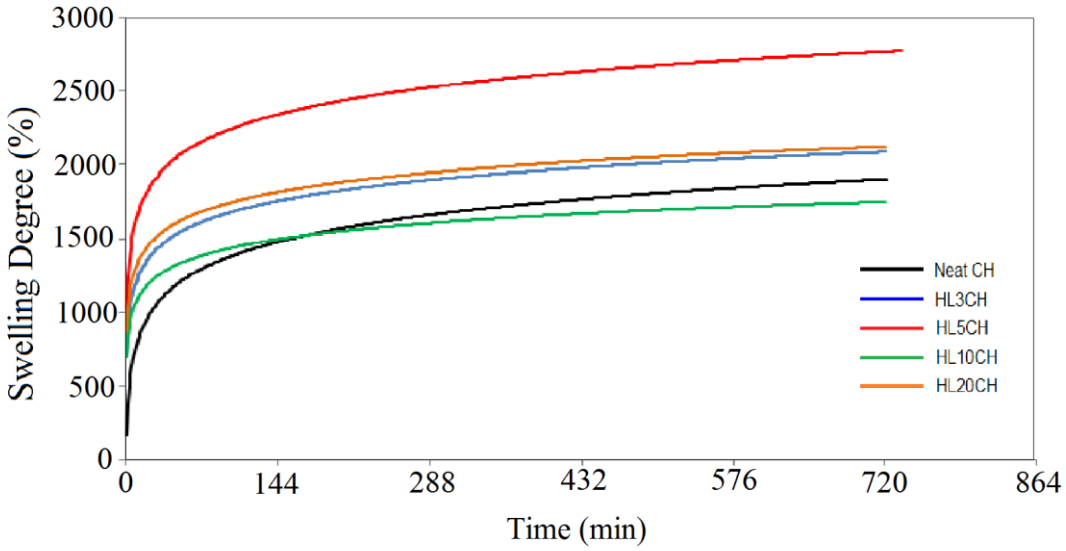

Figure 4.13. Swelling curves for neat chitosan and its composite hydrogels with original halloysite (HL).

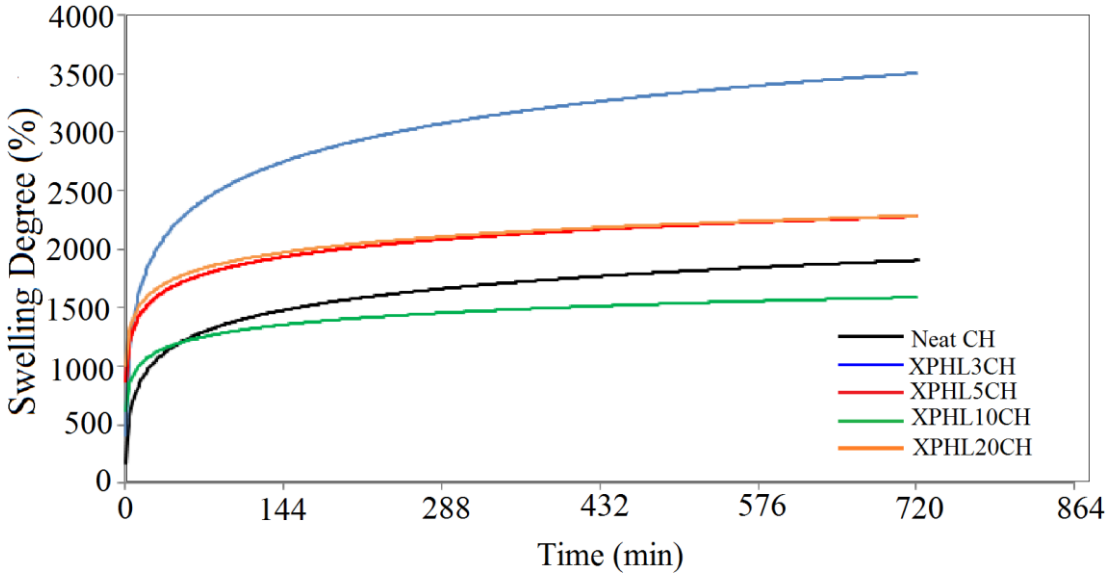

Figure 4.14. Swelling curves for neat chitosan and its composite hydrogels with cryo-expanded halloysite (XPHL).

4.5. Thermal Properties of Chitosan- Halloysite Nanocomposite Hydrogels

The thermal stabilities of neat chitosan, HLCH and XPHLCH hydrogels were investigated by TGA and shown in Figure 4.14 and Figure 4.15.

Maximum peaks, residues at 700 ^{o}C, degradation temperatures at mid-point (T_{d50}) and at 20% (T_{d20}) were given in Table 4.12. Degradation temperatures at 20% (T_{d20}) are higher for all HLCH and XPHLCH hydrogel nanocomposites than neat chitosan. Additionally, the mid-point degradation temperatures (T_{d50}) resulted higher above 10% loading of halloysite. The peak maximum value increases in HLCH and XPHLCH hydrogels due to flame retardancy effect of halloysite [79]. At 20% loading, halloysite containing hydrogels have slower degradation rates at their maximum derivative weight change (%/^{o}C) compared to neat chitosan.

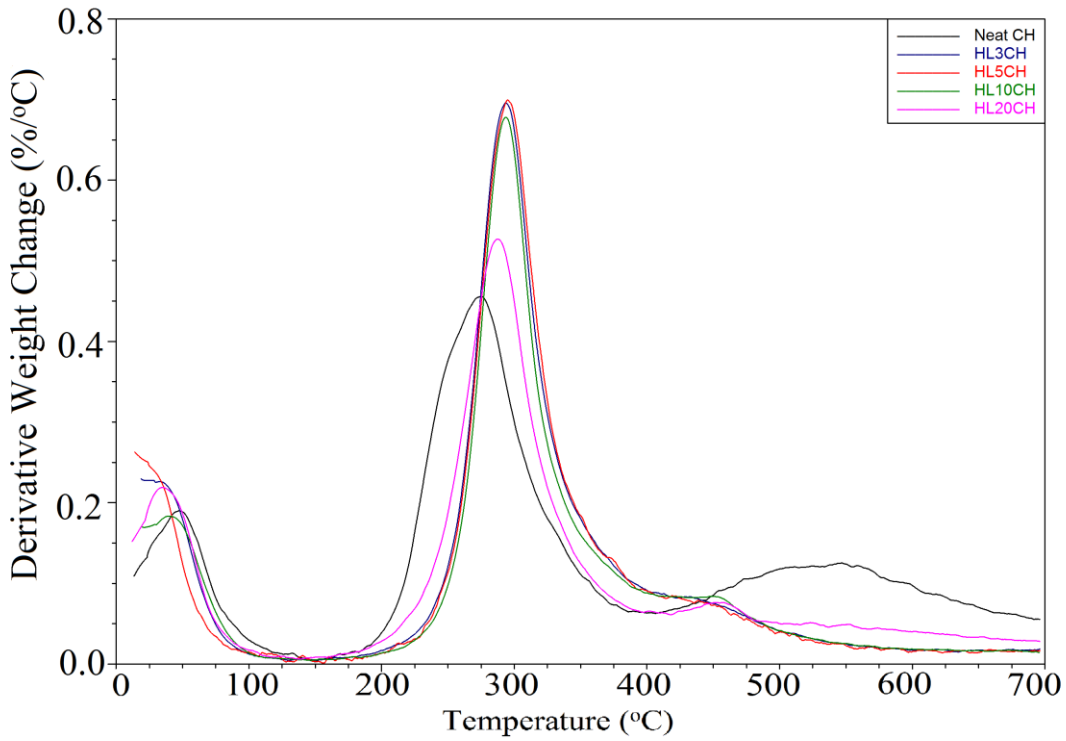

Figure 4.15. TGA derivative thermograms of Neat Chitosan and HLCH hydrogels.

XPHL20CH hydrogel has the highest thermal stability because of the highest increase in T_{d50} value, the highest residue, the lowest degradation rate of 3.199

%.min/ ^{o}C at its maximum peak temperature of 296^{o}C. The increase in T_{d50} and the decrease in degradation rate of XPHLCH hydrogel can be the result of higher interaction between halloysite and chitosan which give rise to formation of physical crosslinks restricting the mobility of polymer chains which causes to slowing down in degradation of cryo-expanded halloysite nanocomposite hydrogels.

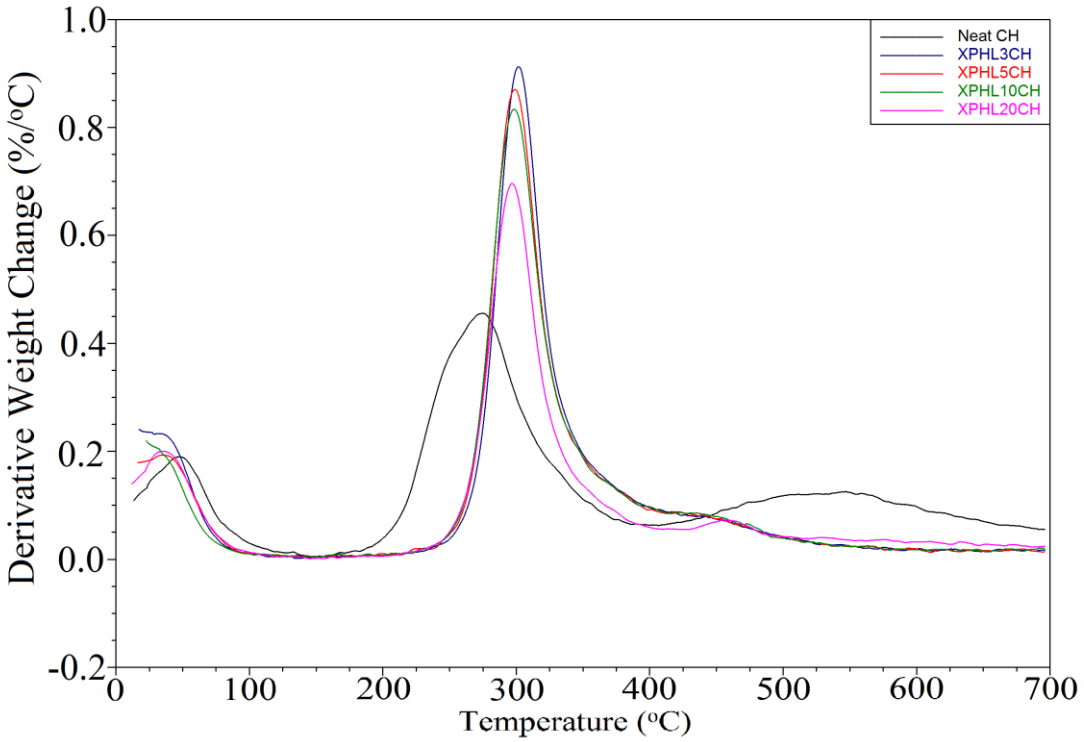

Figure 4.16. TGA derivative thermograms of Neat Chitosan and XPHLCH hydrogels.

Table 4.2. Thermal properties of Neat Chitosan, HLCH and XPHLCH hydrogels.

	Peak Max ($T/^oC$)	Residual Amount (as percentage at 700 ^oC)	T_{20} (Temperature when 20% of the sample is lost)	T_{50} (Temperature when 50% of the sample is lost)
Neat CH	274.68	17.75	246.93	341.13
HL3CH	293.55	28.96	275.39	333.67
XPHL3CH	301.86	27.90	288.27	332.75
HL5CH	295.05	29.35	276.71	333.37
XPHL5CH	299.06	29.47	287.44	337.26
HL10CH	293.61	34.14	280.83	360.44
XPHL10CH	298.42	31.71	289.47	348.35
HL20CH	287.45	32.57	264.47	359.64
XPHL20CH	296.84	38.11	287.16	405.17

4.6. Mechanical Properties of Chitosan-Halloysite Nanocomposite Hydrogels

The wet strengths of neat chitosan and its composite hydrogels were studied in terms of compression test. In Figure 4.16 and Figure 4.17, the compression force-deformation data of HLCH and XPHLCH are shown.

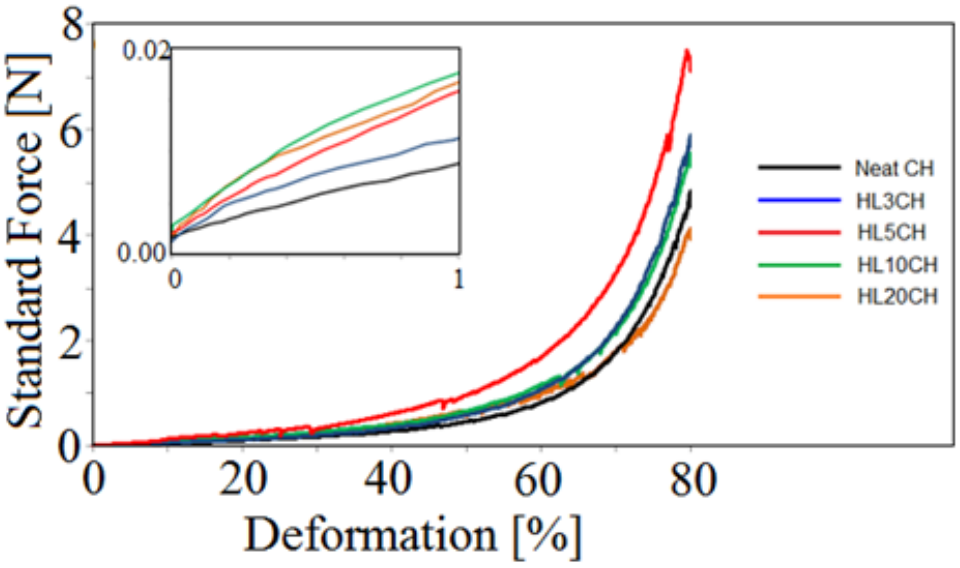

Figure 4.17. Compressive force-deformation curves for neat chitosan and HLCH composite hydrogels. Insert shows an expansion of deformation percentage range of 0-1%, showing compression modulus change of samples.

Neat or composite hydrogels provide high compression strengh without any crack propagation and disintegration. All of the hydrogels remain mechanically stable up to about complete compression (80 %). It should be noted that, all composite hydrogels squeezed under the load, the gel releases all its water so that it is completely compressed. After the release of the load and addition of water, the samples recover their original shape at short notice.

The neat chitosan hydrogel is relatively weak and this restrains its usage if a moderate load bearing capacity is desired. This weakness represents itself in low modulus, compression strength and toughness values. Neat chitosan hydrogel is soft, spongy and elastic. Overall strength and modulus are low, almost 7.85 kPa and 1.18 kPa, respectively. By the addition of HL, compression strength and compression modulus of neat chitosan are improved. Rooj *et al.* reported almost 2-3 fold modulus improvement in hydrogels because of stiff tube like natural halloysite addition [80]. Both two-fold increase in compression strength and toughness values depend on composition up to 5 %, then they decrease. Toughness increases because of non-covalent weak crosslinks between polymer chains and halloysite nanotubes through hydrogen bonds. This interaction leads to a greater

viscous feature and energy dissipation. Nevertheless, the toughness decreases for HL10CH nanocomposite because of much higher modulus resulting from high amount of irregularly dispersed and agglomerated nanotubes that can be observed in SEM images in Figure 4.11c.

However, compression moduli are greater for XPHL reinforced nanocomposite hydrogels than HL hydrogels at 3-5 % loadings. XPHL5CH hydrogel displays 3-fold increase in the compression modulus of neat chitosan as the maximum value among XPHLCH hydrogels.

Above 5 % loading of XPHL nanotube, toughness increases to a maximum value for XPHL10CH with a decrease in the compression modulus, but still higher than most of the other XPHLCH hydrogels. The enhancement of toughness and modulus for XPHL10CH can be attributed to enlarged non-covalent interactions or crosslinks between chitosan and expanded nanotube which leads to a greater uniform dispersion of crosslinking and sub-network (Figure 4.11c) regions especially at cell walls providing stress/energy dissipation.

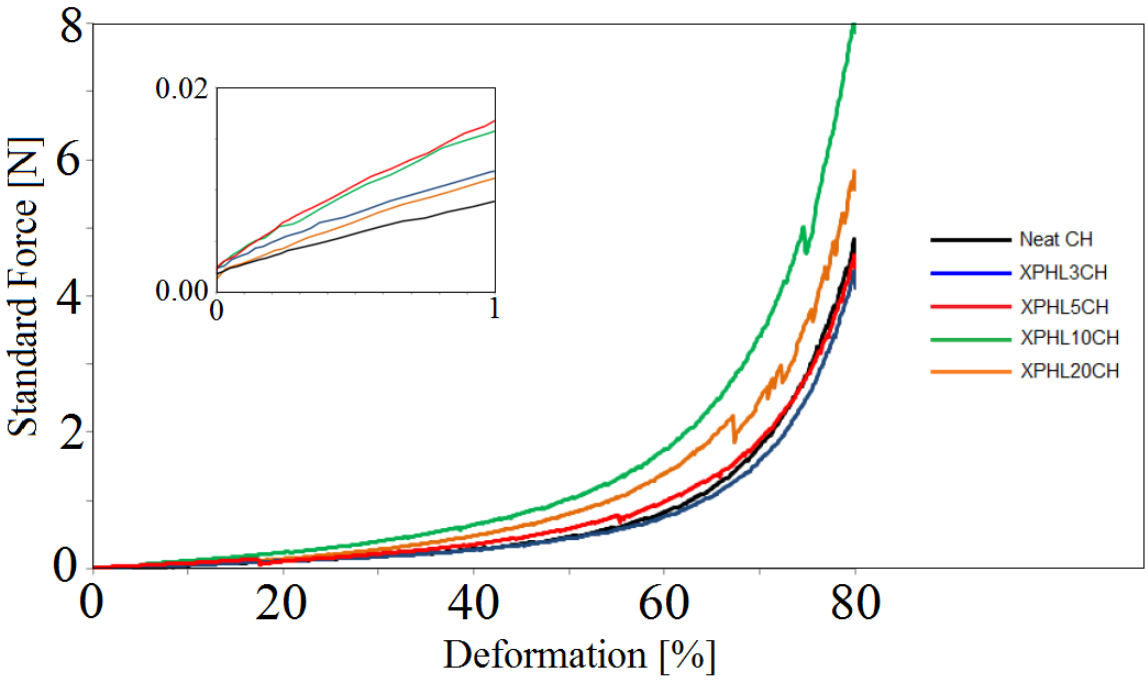

Figure 4.18. Compressive force-deformation curves for neat chitosan and XPHLCH composite hydrogels. Insert shows an expansion of deformation percentage range of 0-1%, showing compression modulus change of the samples.

4.7. Dye Adsorption Capacities of Chitosan-Halloysite Nanocomposite Hydrogels

Removal of dyestuff from waste water has carried attention because of their harmful and toxic nature to human beings and microorganisms. Regarding this polysaccharide based hydrogels are used as dye adsorbents due to their hydrophilic and porous nature. In this project, the adsorption efficiencies of the chitosan and chitosan composite hydrogels were studied for cationic and anionic dyes. Both chitosan and halloysite have many polar and hydrogen bonding sites for chemisorption and also charged sites to lead to adsorption of dyes via electrostatic interactions.

Bromocresol green is an acknowledged anionic dye and adsorption behaviours of the hydrogels for this dye are given in Figure 4.18 and 4.19.

Chitosan is known as a positively charged polysaccharide at low pHs resulting from the protonation of amine sites [73] and it is expected to have an electrostatic attraction with an anionic dye with a high adsorption capacity (16.5 mg/g). Nevertheless, the addition of HL into chitosan matrix causes a decrease in adsorption of BCG up to 6 mg/g because of that the initial negative outer surface charges of halloysite are balanced by chitosan which active sites are consumed of. Comparable results were obtained by Peng et al[34] as well. For cryo-expanded HL loaded hydrogels, the decrease in BCG adsorption capacity is not as much as in HL loaded ones. Dye adsorption increases up to 9 mg/g for XPHL3CH. This outcome can be related to the abundant inner positive charged sites attended as additional active sites with the expansion of nanotubes. Furthermore all composite hydrogels adsorb BCG faster than neat chitosan hydrogel while cryo-expanded hydrogels have superior rates because of the existence of extra numerous active sites resulting from the cryo-expansion.

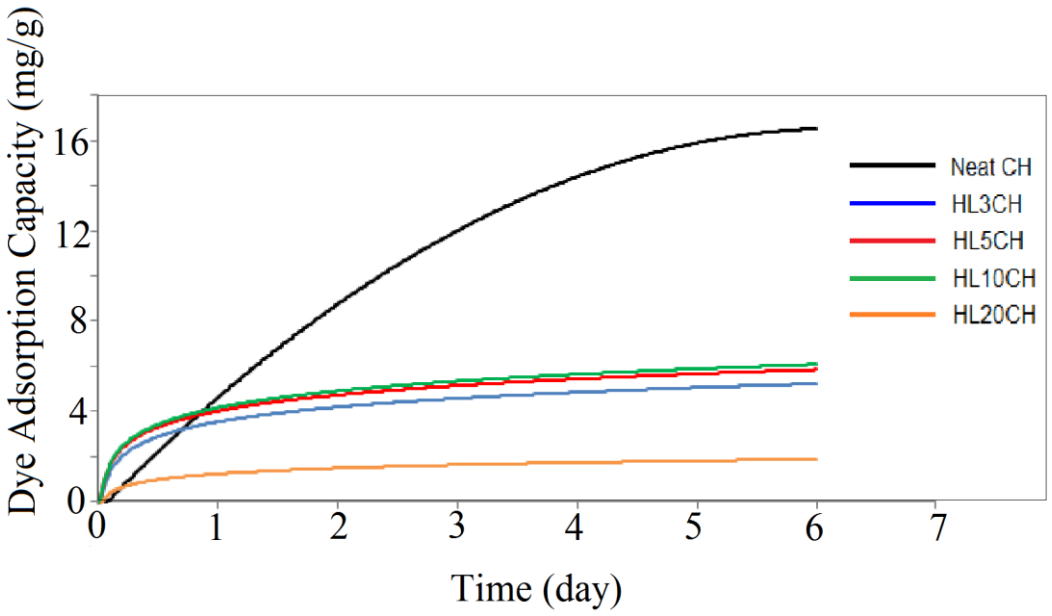

Figure 4.19. The adsorption behaviours of HLCH hydrogels for anionic Bromocresol Green (BCG) dye.

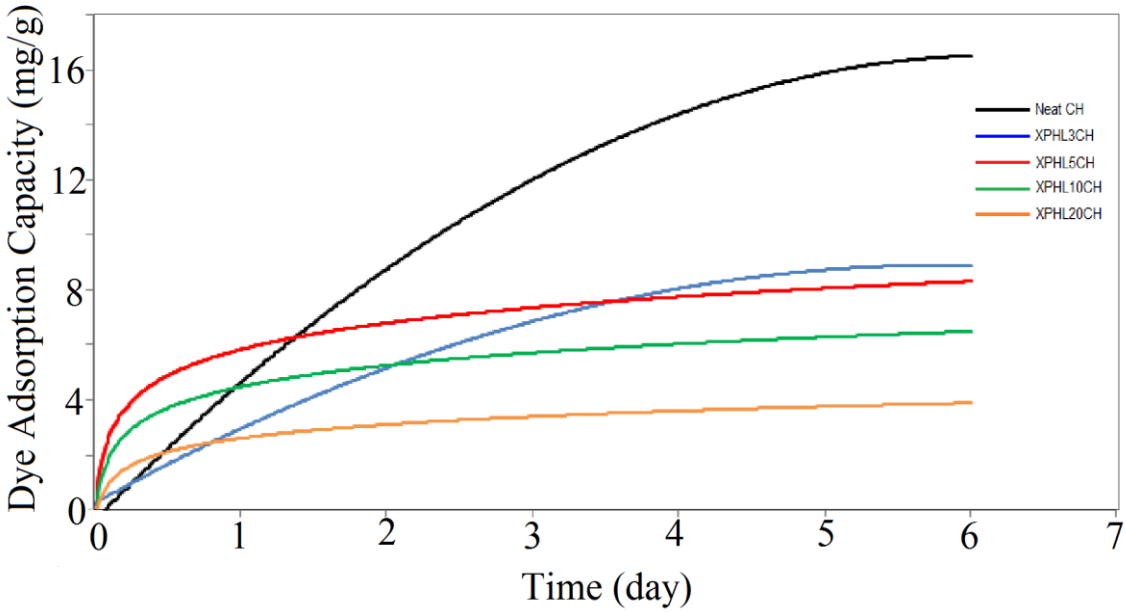

Figure 4.20. The adsorption behaviours of XPHLCH hydrogels for anionic Bromocresol Green (BCG) dye.

The pH of the solution was kept as 5 and it can be observed that in acid aqueous solutions, the amino groups of chitosan are easier to be cationized and they adsorb bromocresol green anions by electrostatic attraction [22]. Also degree of deacetylation

(DD) plays an important role in anionic dye adsorption because of chitin having amide group –CO-NH- that cannot be easily protonated in acidic solutions. Because nitrogen of the amide is a poorer source of electrons via electron withdrawal by carbonyl group [44]. DD of our material is 75-85% and if it was higher, dye adsorption capacity would be higher as well.

Efficient dye adsorption capacity of chitosan hydrogel can be visually followed by the photographs taken during anionic dye adsorption tests (Figure 4.20).

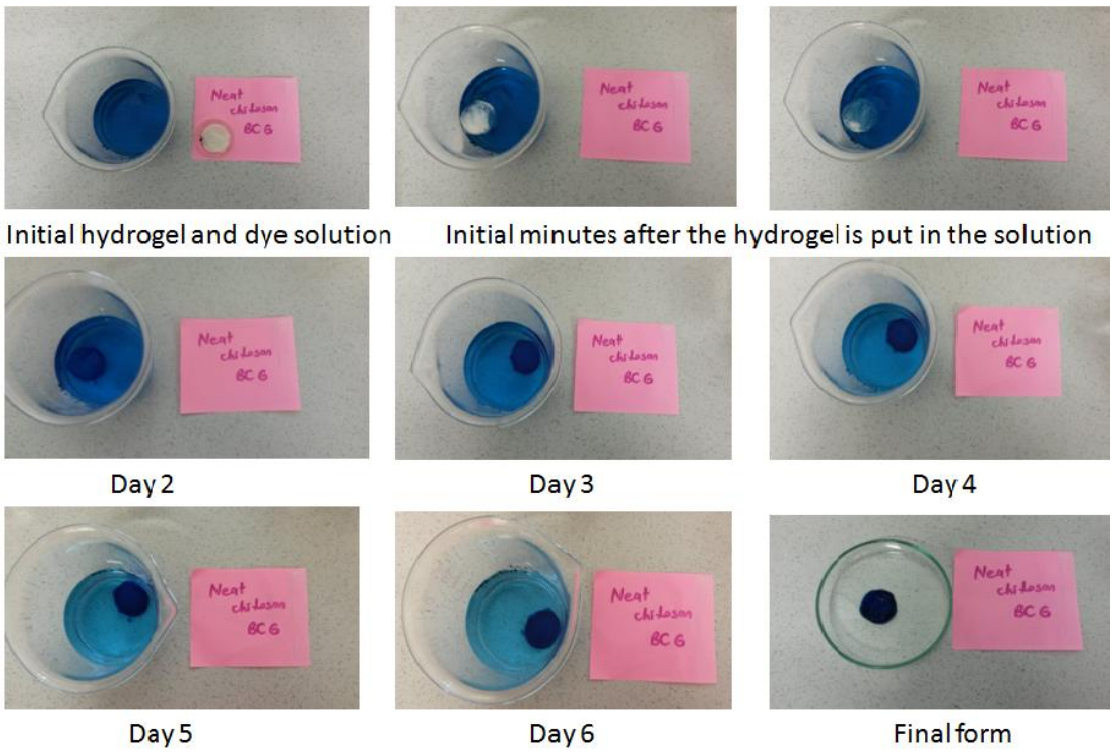

Figure 4.21. Photos of neat chitosan hydrogels during anionic dye adsorption test.

The adsorption behaviour of the hydrogels for Nile Blue chosen as a cationic dye were given in Figure 4.21 and 4.22. Because of the charge discrepancy between chitosan matrix and Nile Blue dye, chitosan still seems as an adsorbent due to the existence of other interactions but with a quite low capacity of 0.4 mg/g .The addition of HL having negative outer surface neutralizes some of the positive charge on chitosan and leaves the structure less positive. Therefore, repulsion between matrix and dye occurs in a limited extent. The average adsorption in HL nanocomposite hydrogels increase up to 3 mg/g.

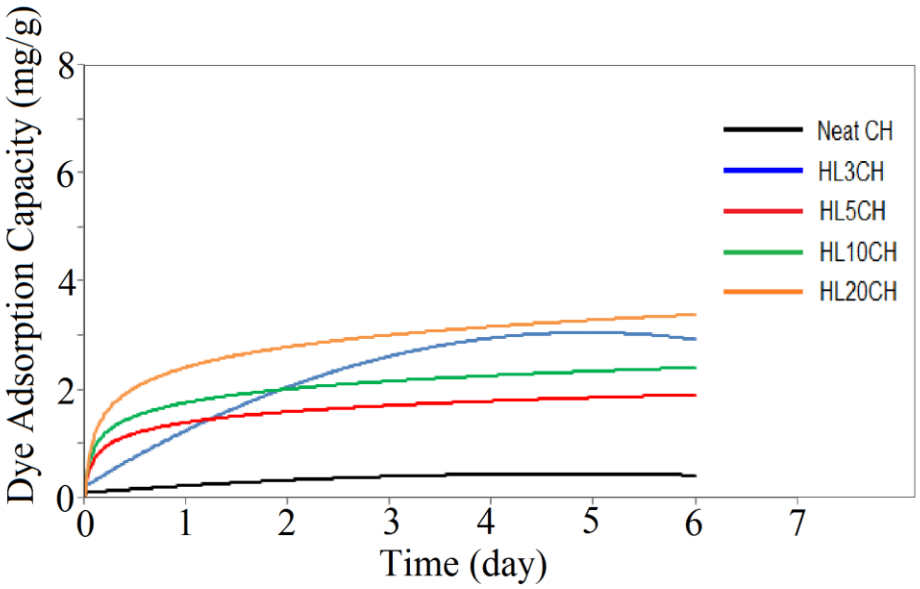

Figure 4.22. The adsorption behaviours of HLCH hydrogels for cationic Nile Blue (NB) dye.

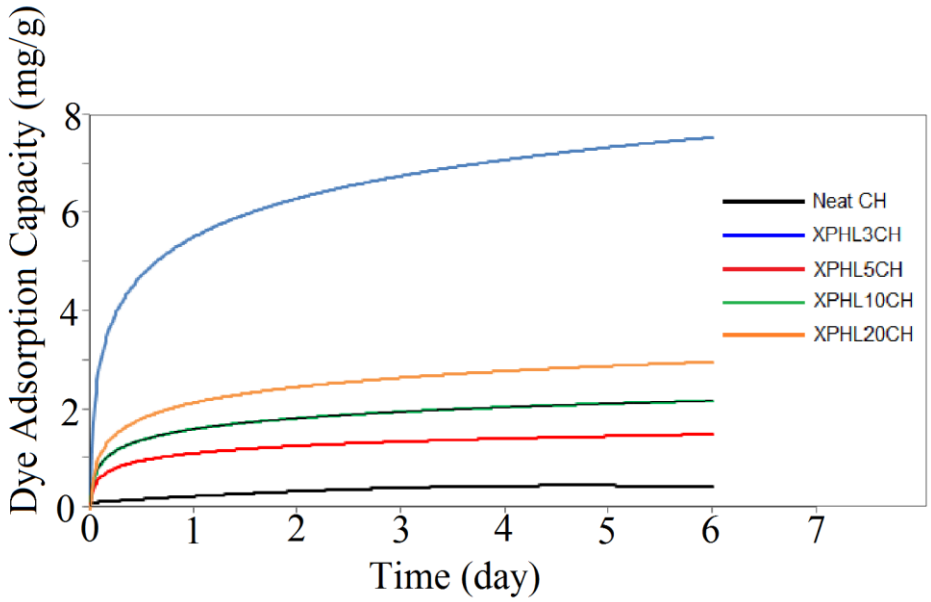

Figure 4.23. The adsorption behaviours of XPHLCH hydrogels for cationic Nile Blue (NB) dye.

However, in XPHL loaded hydrogels additional positive sites created by expansion cause a repulsion which leads to lower adsorption values like 2.5 mg/g. But, it is still higher than neat chitosan hydrogel. Not only electrostatic interactions but also additional effects coming from polar interactions, hydrogen bonding etc. have an influence on dye

adsorption. It is noteworthy that XPHL3CH composition which has maximum swelling (Figure 4.13), has the ultimate adsorption capacity most probably because of the additional special morphology having the active sites in receptor position. This maximum efficiency is given with the photographs taken during adsorption test (Figure 4.23).

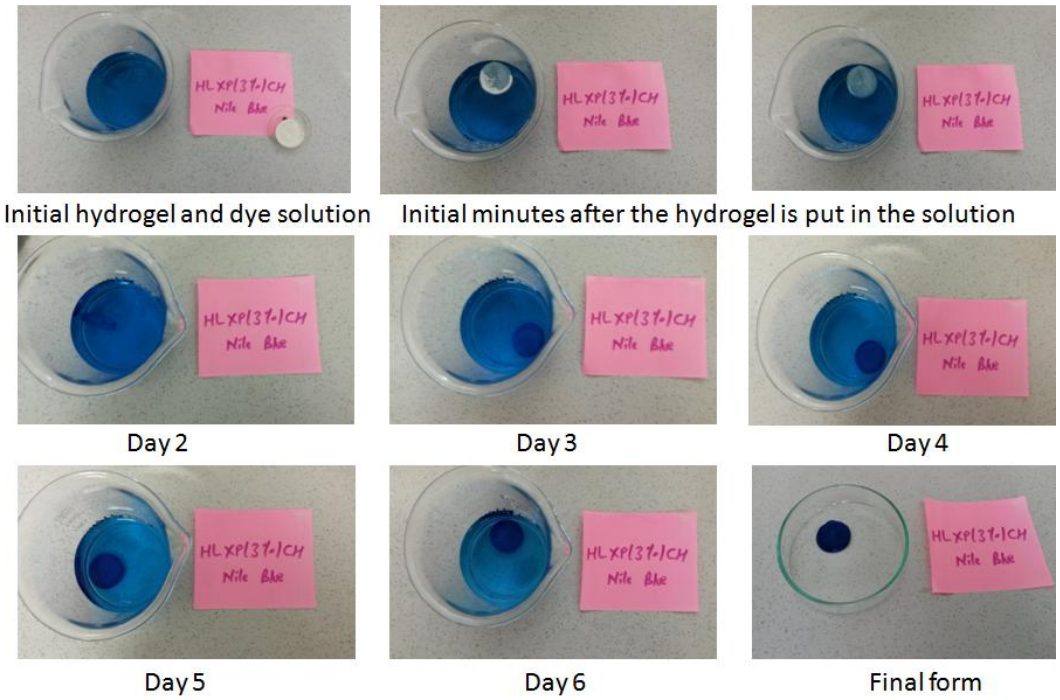

Figure 4.24. Photos of XPHL3CH hydrogels during cationic dye adsorption test.

4.8. Stability, Reusability and Recoverability Studies on Chitosan-Halloysite Hydrogels

In order to see the uncured state stability of the hydrogels, a kind of sedimentation test was performed. Here, the solutions of the chitosan and halloysite with different percentages were prepared, put into graduated cylinders and the volume of the supernatant if any was measured for 10 days. Absence of any kind of sedimentation for four days was accepted as an indication of high suspension stability before regeneration of hydrogel.

Reusability is another important issue in hydrogel studies. For this purpose, first swelling test was conducted with one of hydrogel, XPHL5CH, followed by freezing at -18^{o}C and then freeze-drying. The second swelling test was then applied with this

previously freeze-dried samples. The results given in Fig showed that the hydrogel is still highly water absorptive and moreover is reusable with only 15 % loss.

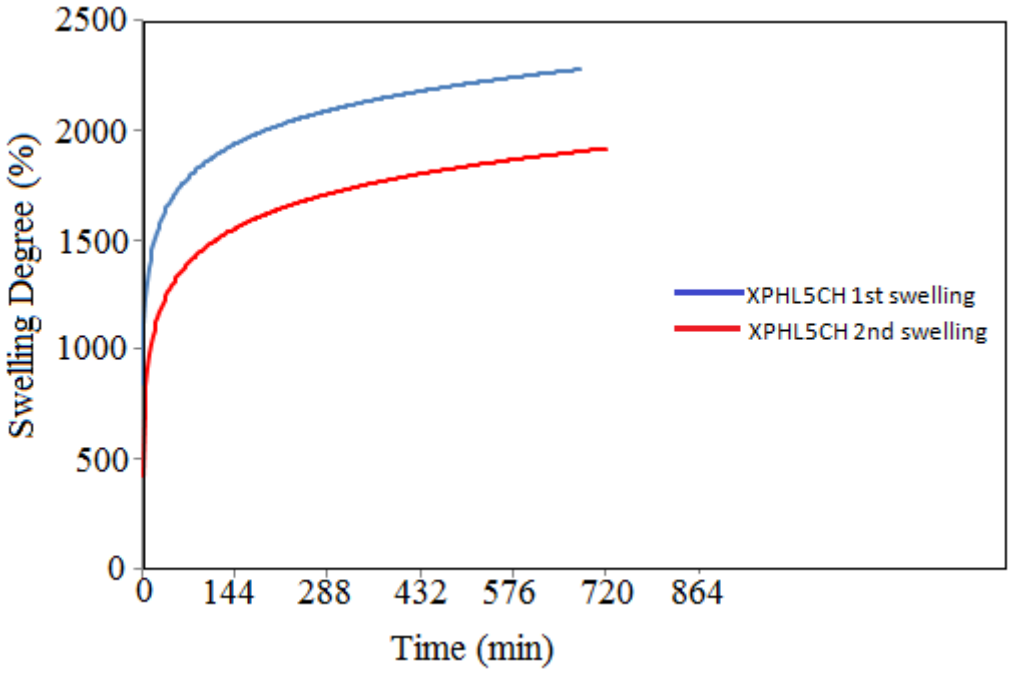

Figure 4.25. Swelling test results for reusability behaviours of XPHL5CH hydrogels.

Regeneration of the dye adsorbed hydrogels can be conducted by desorption method. The dyed hydrogels were washed with first 0.5 M NaOH solution then deionized water and freeze dried. The regenerated hydrogel discs can be observed from the photographs taken after desorption test.

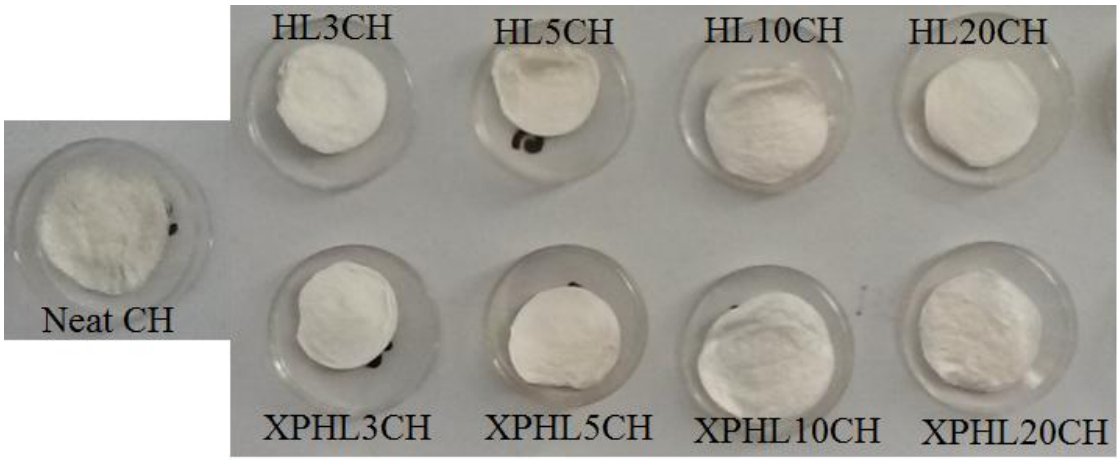

Figure 4.26. Photographs of hydrogels after desorption test of anionic dye adsorption.

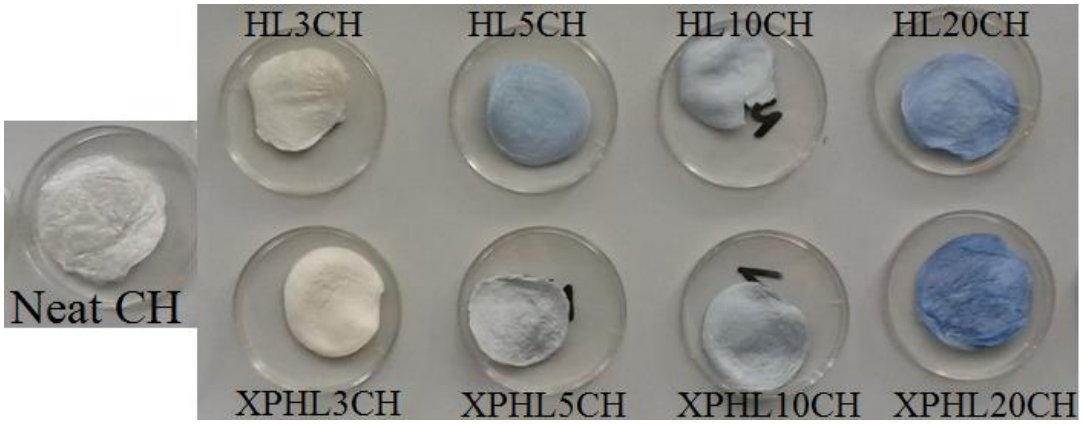

Figure 4.27. Photographs of hydrogels after desorption test of cationic dye adsorption.

The interaction between the dye and the sorbent is known to be driven by electrostatically, hydrophobically and via ion-exchange [70]. It is clear that all compositions having both halloysite and cryo-expanded halloysite desorped the anionic Bromocresol Green succsesfully without leaving any color behind. It is probably due to the anionic character of BCG, matrix chitosan already adsorbed it dominantly whereas tight halloysites serve only their surface hydroxides rather than lumen cations, desorption occurs easily. On the other hand, the hydrogels having both type of halloysite above 3% didn't release Nile Blue efficiently. Chen *et al.* reported that since the strong coordination between nitrogen of amino group in dyes and aluminum of inner lumens exist, the removal efficiency decreases [70]. In our case, the formation of such coordination between nitrogen and lumen alumina is expected also. It is worth to say that these new class dye adsorbers can be reused for further water and dye sorption studies efficiently.

5. CONCLUSION

In this thesis, a novel method based on a cryogenic technique for expansion of the halloysite nanotubes was studied. BET, SEM and XRD analyses confirmed that the inner-outer diameters and the surface area of halloysite nanotubes can increase without disturbing the inherent tubular structure. Additionally, composite hydrogels were formed from chitosan with original and cryo-expanded nanotubes and characterization of these nanocomposites in terms of morphology, water absorption, compressive strength and dye adsorption properties. The resultant hydrogels were investigated by the SEM technique. It was resulted that neat chitosan hydrogels obtained irregular microchannel-like porosity which changes into open-cell morphology in the presence of original and cryo-expanded halloysite.

Furthermore, hydrogels having 5% original and 3% cryo-expanded halloysite had the most uniform cell distribution. Swelling studies showed that the maximum swelling in neat chitosan hydrogel is 1750%, however, it increases in original and cryo-expanded halloysite containing hydrogels. In spite of the fact that, the maximum swelling occurs at 5% HL loading, this value decreases to a 3% loading for cryo-expanded halloysite in the nanocomposite hydrogels. Wet compression strength, compressive modulus and toughness values increased for composite hydrogels compared to neat chitosan depending on the compositon. This feature was observed for hydrogels containing cryo-expanded halloysite nanotubes. Anionic and cationic dye adsorption studies showed that neat chitosan is a good adsorbent for anionic dyes. Moreover, the composite hydrogel containing cryo-expanded halloysite in three percentages can exhibit a high adsorption capacity for both types of dyes.

To sum up, producing a multiselective waste water treatment material that has high water absorption, multi-charged dye adsorption and compression resistivity was experimented successfully by using natural polymers, natural silica nanotubes and cryo-expanded silica nanotubes.

REFERENCES

1. Berger J., Reist M., Mayer J. M., Felt O., Peppas N. a., and Gurny R., "Structure and interactions in covalently and ionically crosslinked chitosan hydrogels for biomedical applications", *European Journal of Pharmaceutics and Biopharmaceutics*, Vol. 57, pp. 19–34, 2004.

2. Ahmed E. M., "Hydrogel: Preparation, characterization, and applications", *Journal of Advanced Research*, Vol. 6, No. 2, pp. 105–121, 2013.

3. Ebara M., Y. Kotsuchibashi, R. Narain, N. Idota, Y.-J. Kim, J. M. Hoffman, K. Uto, and T. Aoyagi, *Smart Biomaterials*. 2014.

4. Hussain T., M. Ansari, N. M. Ranjha, I. U. Khan, and Y. Shahzad, "Chemically cross-Linked poly(acrylic- Co -Vinylsulfonic) acid hydrogel for the delivery of isosorbide mononitrate", *The Scientific World Journal*, Vol. 2013, 2013.

5. Xue W., M. B. Huglin, and T. G. J. Jones, "Swelling and network parameters of crosslinked thermoreversible hydrogels of poly(N-ethylacrylamide)", *European Polymer Journal*, Vol. 41, pp. 239–248, 2005.

6. Kamoun E. a., E. R. S. Kenawy, T. M. Tamer, M. a. El-Meligy, and M. S. Mohy Eldin, "Poly (vinyl alcohol)-alginate physically crosslinked hydrogel membranes for wound dressing applications: Characterization and bio-evaluation", *Arabian Journal of Chemistry*, Vol. 8, No. 1, pp. 38–47, 2013.

7. Niu H., F. Wang, and R. a. Weiss, "Hydrophobic/Hydrophilic Triblock Copolymers: Synthesis and Properties of Physically Cross-Linked Hydrogels", *Macromolecules*, Vol. 48, pp. 645–654, 2015.

8. Pekel N., F. Yoshii, T. Kume, and O. Güven, "Radiation crosslinking of biodegradable hydroxypropylmethylcellulose", *Carbohydrate Polymers*, Vol. 55, pp. 139–147, 2004.

9. Gibas I. and H. Janik, “Review : Synthetic Polymer Hydrogels for Biomedical”, *Chemical Technology*, Vol. 4, No. 4, pp. 297–304, 2010.

10. Hua F., M. Qian, “Synthesis of self-crosslinking sodium polyacrylate hydrogel and water-absorbing mechanism”, *Journal of Materials Science*, Vol. 36, pp. 731–738, 2001.

11. Sengupta R., S. Chakraborty, S. Bandyopadhyay, S. Dasgupta, R. Mukhopadhyay, K. Auddy, and a S. Deuri, “A Short Review on Rubber / Clay Nanocomposites With Emphasis on Mechanical Properties”, *Engineering*, Vol. 47, pp. 21–25, 2007.

12. Tan H., K. G. Marra, “Injectable, biodegradable hydrogels for tissue engineering applications”, *Materials*, Vol. 3, pp. 1746–1767, 2010.

13. Patenaude M., T. Hoare, “Injectable, mixed natural-synthetic polymer hydrogels with modular properties”, *Biomacromolecules*, Vol. 13, pp. 369–378, 2012.

14. Sadeghi M., “Synthesis of pH-Sensitive Hydrogel Based on Starch-Polyacrylate Superabsorbent”, *Journal of Biomaterials and Nanobiotechnology*, Vol. 03, No. May, pp. 310–314, 2012.

15. Prashanth K. V., R. N. Tharanathan, “Chitin/chitosan: modifications and their unlimited application potential-an overview”, *Trends in Food Science and Technology*, Vol. 18, pp. 117–131, 2007.

16. Yi H., L. Q. Wu, W. E. Bentley, R. Ghodssi, G. W. Rubloff, J. N. Culver, and G. F. Payne, “Biofabrication with chitosan”, *Biomacromolecules*, Vol. 6, No. 6, pp. 2881–2894, 2005.

17. Peniche C., W. Argüelles-Monal, “Overview on structural characterization of chitosan molecules in relation with their behavior in solution”, *Macromolecular Symposia*, Vol. 168, pp. 1–20, 2001.

18. Guibal E., “Heterogeneous catalysis on chitosan-based materials: A review”, *Progress in Polymer Science (Oxford)*, Vol. 30, pp. 71–109, 2005.

19. Mucha M., A. Pawlak, “Thermal analysis of chitosan and its blends”, *Thermochimica Acta*, Vol. 427, pp. 69–76, 2005.

20. Sashiwa H., S. I. Aiba, “Chemically modified chitin and chitosan as biomaterials”, *Progress in Polymer Science (Oxford)*, Vol. 29, pp. 887–908, 2004.

21. Crini G., “Recent developments in polysaccharide-based materials used as adsorbents in wastewater treatment”, *Progress in Polymer Science (Oxford)*, Vol. 30, pp. 38–70, 2005.

22. Cestari A. R., E. F. S. Vieira, A. G. P. Dos Santos, J. a. Mota, and V. P. De Almeida, “Adsorption of anionic dyes on chitosan beads. 1. The influence of the chemical structures of dyes and temperature on the adsorption kinetics”, *Journal of Colloid and Interface Science*, Vol. 280, pp. 380–386, 2004.

23. Liu M., Y. Zhang, J. Li, and C. Zhou, “Chitin-natural clay nanotubes hybrid hydrogel”, *International Journal of Biological Macromolecules*, Vol. 58, pp. 23–30, 2013.

24. Mi F. L., S. S. Shyu, C. T. Chen, and J. Y. Lai, “Adsorption of indomethacin onto chemically modified chitosan beads”, *Polymer*, Vol. 43, pp. 757–765, 2001.

25. Mcafee B., W. Gould, J. Nadeau, and A. da Costa, “Biosorption of Metal Ions Using Chitosan, Chitin, and Biomass of Rhizopus Oryzae”, *Separation Science and Technology*, Vol. 36, No. February 2015, pp. 3207–3222, 2001.

26. Kim B. S., S.-T. Lim, “Removal of heavy metal ions from water by cross-linked carboxymethyl corn starch”, *Carbohydrate Polymers*, Vol. 39, pp. 217–223, 1999.

27. Seidel C., W. M. Kulicke, C. Heß, B. Hartmann, M. D. Lechner, and W. Lazik, “Influence of the cross-linking agent on the gel structure of starch derivatives”, *Starch/Staerke*, Vol. 53, pp. 305–310, 2001.

28. Prashanth K. V., R. N. Tharanathan, “Crosslinked chitosan - Preparation and characterization”, *Carbohydrate Research*, Vol. 341, pp. 169–173, 2006.

29. Chung H. J., K. S. Woo, and S. T. Lim, “Glass transition and enthalpy relaxation of cross-linked corn starches”, *Carbohydrate Polymers*, Vol. 55, pp. 9–15, 2004.

30. Sakurai K., T. Maegawa, and T. Takahashi, “Glass transition temperature of chitosan and miscibility of chitosan / poly (N-vinyl pyrrolidone) blends”, *Materials Science*, Vol. 41, pp. 7051–7056, 2000.

31. Demir A., N. Seventekin, “Kitin, Kitosan ve Genel Kullanım Alanları”, *Teknolojik Araştırmalar*, Vol. 3, No. 2, pp. 92–103, 2009.

32. Mourya V. K., N. N. Inamdar, “Chitosan-modifications and applications: Opportunities galore”, *Reactive and Functional Polymers*, Vol. 68, pp. 1013–1051, 2008.

33. Hamman J. H., “Chitosan based polyelectrolyte complexes as potential carrier materials in drug delivery systems”, *Marine Drugs*, Vol. 8, pp. 1305–1322, 2010.

34. Peng Q., M. Liu, J. Zheng, and C. Zhou, “Microporous and Mesoporous Materials Adsorption of dyes in aqueous solutions by chitosan – halloysite nanotubes composite hydrogel beads”, *Microporous and Mesoporous Materials*, Vol. 201, pp. 190–201, 2015.

35. Hashimoto M., M. Morimoto, H. Saimoto, Y. Shigemasa, and T. Sato, “Lactosylated chitosan for DNA delivery into hepatocytes: The effect of lactosylation on the physicochemical properties and intracellular trafficking of pDNA/chitosan complexes”, *Bioconjugate Chemistry*, Vol. 17, No. Scheme 1, pp. 309–316, 2006.

36. Shirosaki Y., K. Tsuru, S. Hayakawa, A. Osaka, M. A. Lopes, J. D. Santos, and M. H. Fernandes, “In vitro cytocompatibility of MG63 cells on chitosan-organosiloxane hybrid membranes”, *Biomaterials*, Vol. 26, pp. 485–493, 2005.

37. Thanou M., J. C. Verhoef, and H. E. Junginger, “Oral drug absorption enhancement by chitosan and its derivatives”, *Advanced Drug Delivery Reviews*, Vol. 52, pp. 117–126, 2001.

38. Sadeghi M. M., F. a. Dorkoosh, M. R. Avadi, P. Saadat, M. Rafiee-Tehrani, and H. E. Junginger, "Preparation, characterization and antibacterial activities of chitosan, N-trimethyl chitosan (TMC) and N-diethylmethyl chitosan (DEMC) nanoparticles loaded with insulin using both the ionotropic gelation and polyelectrolyte complexation methods", *International Journal of Pharmaceutics*, Vol. 355, pp. 299–306, 2008.

39. Qin C., H. Li, Q. Xiao, Y. Liu, J. Zhu, and Y. Du, "Water-solubility of chitosan and its antimicrobial activity", *Carbohydrate Polymers*, Vol. 63, pp. 367–374, 2006.

40. Pillai C. K. S., W. Paul, and C. P. Sharma, "Chitin and chitosan polymers: Chemistry, solubility and fiber formation", *Progress in Polymer Science (Oxford)*, Vol. 34, pp. 641–678, 2009.

41. Wang P. Su, C., X. Yang, X. Chen, C. Gao, X. X. Feng, J. Y. Chen, J. Ye, and Z. Gou, "Electrospinning of chitosan nanofibers: The favorable effect of metal ions", *Carbohydrate Polymers*, Vol. 84, pp. 239–246, 2011.

42. Test S., "A Comparative Study on Metal Adsorption Properties of Different Forms of Chitosan", Vol. 3, No. 2, pp. 9609–9617, 2014.

43. Kurita K., "Controlled functionalization of the polysaccharide chitin", *Progress in Polymer Science (Oxford)*, Vol. 26, pp. 1921–1971, 2001.

44. Chiou M. S., P. Y. Ho, and H. Y. Li, "Adsorption of anionic dyes in acid solutions using chemically cross-linked chitosan beads", *Dyes and Pigments*, Vol. 60, pp. 69–84, 2004.

45. Ray M., K. Pal, a. Anis, and a. K. Banthia, "Development and Characterization of Chitosan-Based Polymeric Hydrogel Membranes", *Designed Monomers & Polymers*, Vol. 13, No. 3, pp. 193–206, 2010.

46. Hong Y., H. Song, Y. Gong, Z. Mao, C. Gao, and J. Shen, "Covalently crosslinked chitosan hydrogel: Properties of in vitro degradation and chondrocyte encapsulation", *Acta Biomaterialia*, Vol. 3, No. 1, pp. 23–31, 2007.

47. Kufelt O., A. El-Tamer, C. Sehring, M. Meißner, S. Schlie-Wolter, and B. N. Chichkov, “Water-soluble photopolymerizable chitosan hydrogels for biofabrication via two-photon polymerization”, *Acta Biomaterialia*, 2015.

48. Mahdavinia G. R., a. Pourjavadi, and M. J. Zohuriaan-Mehr, “A convenient one-step preparation of chitosan-poly(sodium acrylate-co-acrylamide) hydrogel hybrids with super-swelling properties”, *Journal of Applied Polymer Science*, Vol. 99, No. 4, pp. 1615–1619, 2006.

49. Thein-Han W. W., R. D. K. Misra, “Biomimetic chitosan-nanohydroxyapatite composite scaffolds for bone tissue engineering”, *Acta Biomaterialia*, Vol. 5, No. 4, pp. 1182–1197, 2009.

50. Majeed K., M. Jawaid, a. Hassan, a. Abu Bakar, H. P. S. Abdul Khalil, a. a. Salema, and I. Inuwa, “Potential materials for food packaging from nanoclay/natural fibres filled hybrid composites”, *Materials and Design*, Vol. 46, pp. 391–410, 2013.

51. Spitalsky Z., D. Tasis, K. Papagelis, and C. Galiotis, “Carbon nanotube-polymer composites: Chemistry, processing, mechanical and electrical properties”, *Progress in Polymer Science (Oxford)*, Vol. 35, No. 3, pp. 357–401, 2010.

52. Singh S., H. Mahalingam, and P. K. Singh, “Polymer-supported titanium dioxide photocatalysts for environmental remediation: A review”, *Applied Catalysis A: General*, Vol. 462–463, pp. 178–195, 2013.

53. Potts J. R., D. R. Dreyer, C. W. Bielawski, and R. S. Ruoff, “Graphene-based polymer nanocomposites”, *Polymer*, Vol. 52, No. 1, pp. 5–25, 2011.

54. Sawant S. N., V. Selvaraj, V. Prabhawathi, and M. Doble, “Antibiofilm Properties of Silver and Gold Incorporated PU, PCLm, PC and PMMA Nanocomposites under Two Shear Conditions”, *PLoS ONE*, Vol. 8, No. 5, pp. 1–9, 2013.

55. Vymazalova Z., P. Hron, “Polymer composites silicone rubber-hydrogel”, *Kautschuk Gummi Kunststoffe*, Vol. 54, No. 5, pp. 230–234, 2001.

56. Chang M. C., C. C. Ko, and W. H. Douglas, “Preparation of hydroxyapatite-gelatin nanocomposite”, *Biomaterials*, Vol. 24, pp. 2853–2862, 2003.

57. Biosci I. J., H. F. Jirandehi, and Z. Alimardan, “Synthesis of chitosan based hydrogel nanocomposite for controlled release of cisplatin drug”, Vol. 6655, pp. 92–98, 2014.

58. Govindan S., E. a. K. Nivethaa, R. Saravanan, V. Narayanan, and a. Stephen, “Synthesis and characterization of chitosan–silver nanocomposite”, *Applied Nanoscience*, Vol. 2, pp. 299–303, 2012.

59. Ece O., I. and P. a. Schroeder, “Clay mineralogy and chemistry of halloysite and alunite deposits in the Turplu area, Balikesir, Turkey”, *Clays and Clay Minerals*, Vol. 55, No. 1, pp. 18–35, 2007.

60. White R. D., D. V. Bavykin, and F. C. Walsh, “The stability of halloysite nanotubes in acidic and alkaline aqueous suspensions”, Vol. 065705, 2012.

61. Kamble R., M. Ghag, S. Gaikawad, and B. K. Panda, “Review article halloysite nanotubes and applications : A review”, *Journal of Advanced Scientific Research*, Vol. 3, No. 2, pp. 25–29, 2012.

62. Rawtani D., Y. K. Agrawal, “Multifarious applications of halloysite nano tubes: a review”, *Reviews on Advanced Materials Science*, Vol. 30, pp. 282–295, 2012.

63. Irani M., H. Ismail, and Z. Ahmad, “Hydrogel composites based on linear low-density polyethylene-g-poly (acrylic acid)/kaolin or halloysite nanotubes”, *Journal of Applied Polymer Science*, Vol. 131, pp. 1–11, 2014.

64. Du M., M. Du, B. Guo, B. Guo, X. Cai, X. Cai, Z. Jia, Z. Jia, M. Liu, M. Liu, D. Jia, and D. Jia, “Morphology and properties of halloysite reinforced polypropylene nanocomposites nanotubes”, *Polymer*, No. 130, pp. 1–14, 2008.

65. Cervini-Silva J., A. Nieto-Camacho, E. Palacios, J. A. Montoya, V. Gómez-Vidales, and M. T. Ramírez-Apán, “Anti-inflammatory and anti-bacterial activity, and CYTOTOXICITY of halloysite surfaces”, *Colloids and Surfaces B: Biointerfaces*, Vol. 111, pp. 651–655, 2013.

66. Lin X., X. Ju, R. Xie, M. Jiang, J. Wei, and L. Chu, “Halloysite nanotube composited thermo-responsive hydrogel system for controlled-release”, *Chinese Journal of Chemical Engineering*, Vol. 21, No. 9, pp. 991–998, 2013.

67. Tu J., Z. Cao, Y. Jing, C. Fan, C. Zhang, L. Liao, and L. Liu, “Halloysite nanotube nanocomposite hydrogels with tunable mechanical properties and drug release behavior”, *Composites Science and Technology*, Vol. 85, pp. 126–130, 2013.

68. Pal P., M. K. Kundu, A. Malas, and C. K. Das, “Compatibilizing effect of halloysite nanotubes in polar-nonpolar hybrid system”, *Journal of Applied Polymer Science*, Vol. 131, 2014.

69. Yuan P., P. D. Southon, Z. Liu, and C. J. Kepert, “Organosilane functionalization of halloysite nanotubes for enhanced loading and controlled release”, *Nanotechnology*, Vol. 23, p. 375705, 2012.

70. Chen H., J. Zhao, J. Wu, and H. Yan, “RSC Advances Selective desorption characteristics of halloysite nanotubes for anionic azo dyes †”, No. c, pp. 15389–15393, 2014.

71. Tang Y., S. Deng, L. Ye, C. Yang, Q. Yuan, J. Zhang, and C. Zhao, “Effects of unfolded and intercalated halloysites on mechanical properties of halloysite-epoxy nanocomposites”, *Composites Part A: Applied Science and Manufacturing*, Vol. 42, No. 4, pp. 345–354, 2011.

72. Abdullayev E., A. Joshi, W. Wei, Y. Zhao, and Y. Lvov, “Enlargement of halloysite clay nanotube lumen by selective etching of aluminum oxide”, *ACS Nano*, Vol. 6, No. 8, pp. 7216–7226, 2012.

73. Liu M., Y. Zhang, C. Wu, S. Xiong, and C. Zhou, “Chitosan/halloysite nanotubes bionanocomposites: Structure, mechanical properties and biocompatibility”, *International Journal of Biological Macromolecules*, Vol. 51, No. 4, pp. 566–575, 2012.

74. Liu M., C. Wu, Y. Jiao, S. Xiong, and C. Zhou, "Chitosan–halloysite nanotubes nanocomposite scaffolds for tissue engineering", *Journal of Materials Chemistry B*, Vol. 1, p. 2078, 2013.

75. Yuan P., P. D. Southon, Z. Liu, M. E. R. Green, J. M. Hook, S. J. Antill, and C. J. Kepert, "Functionalization of halloysite clay nanotubes by grafting with aminopropyltriethoxysilane", *Journal of Physical Chemistry C*, Vol. 112, pp. 15742–15751, 2008.

76. Sing K. S. W., "Reporting physisorption data for gas/solid systems with special reference to the determination of surface area and porosity (Recommendations 1984)", *Pure and Applied Chemistry*, Vol. 57, No. 11, pp. 603–619, 1985.

77. Aranaz I., M. Gutiérrez, M. Ferrer, and F. del Monte, "Preparation of Chitosan Nanocompositeswith a Macroporous Structure by Unidirectional Freezing and Subsequent Freeze-Drying", *Marine Drugs*, Vol. 12, pp. 5619–5642, 2014.

78. Daly R. C., C. A. Fleischer, A. L. Wagner, M. Duffy, and S. Place, "Halloysite Nanotubes in Polymers", *Natural Nano*, Vol. 1, pp. 187–190, 2008.

79. Zhao J., C. L. Deng, S. L. Du, L. Chen, C. Deng, and Y. Z. Wang, "Synergistic flame-retardant effect of halloysite nanotubes on intumescent flame retardant in LDPE", *Journal of Applied Polymer Science*, Vol. 131, pp. 8–11, 2014.

80. Rooj S., A. Das, and G. Heinrich, "Tube-like natural halloysite/fluoroelastomer nanocomposites with simultaneous enhanced mechanical, dynamic mechanical and thermal properties", *European Polymer Journal*, Vol. 47, No. 9, pp. 1746–1755, 2011.